



Coupled MBS-FE Applications

A New Trend in Simulation

Michel Géradin
Emeritus Professor
University of Liège, Belgium



Outline

- Introduction.
- General kinematics.
- Flexible MBS: a first series of examples.
- General formulation: variational approach, implicit solution methodology.
- Joint modeling: from functional to mesoscopic representation.
- Modal synthesis in multibody dynamics.
- Co-simulation.
- Conclusions.



Introduction

Coupled MBS – FE applications

A new trend in simulation

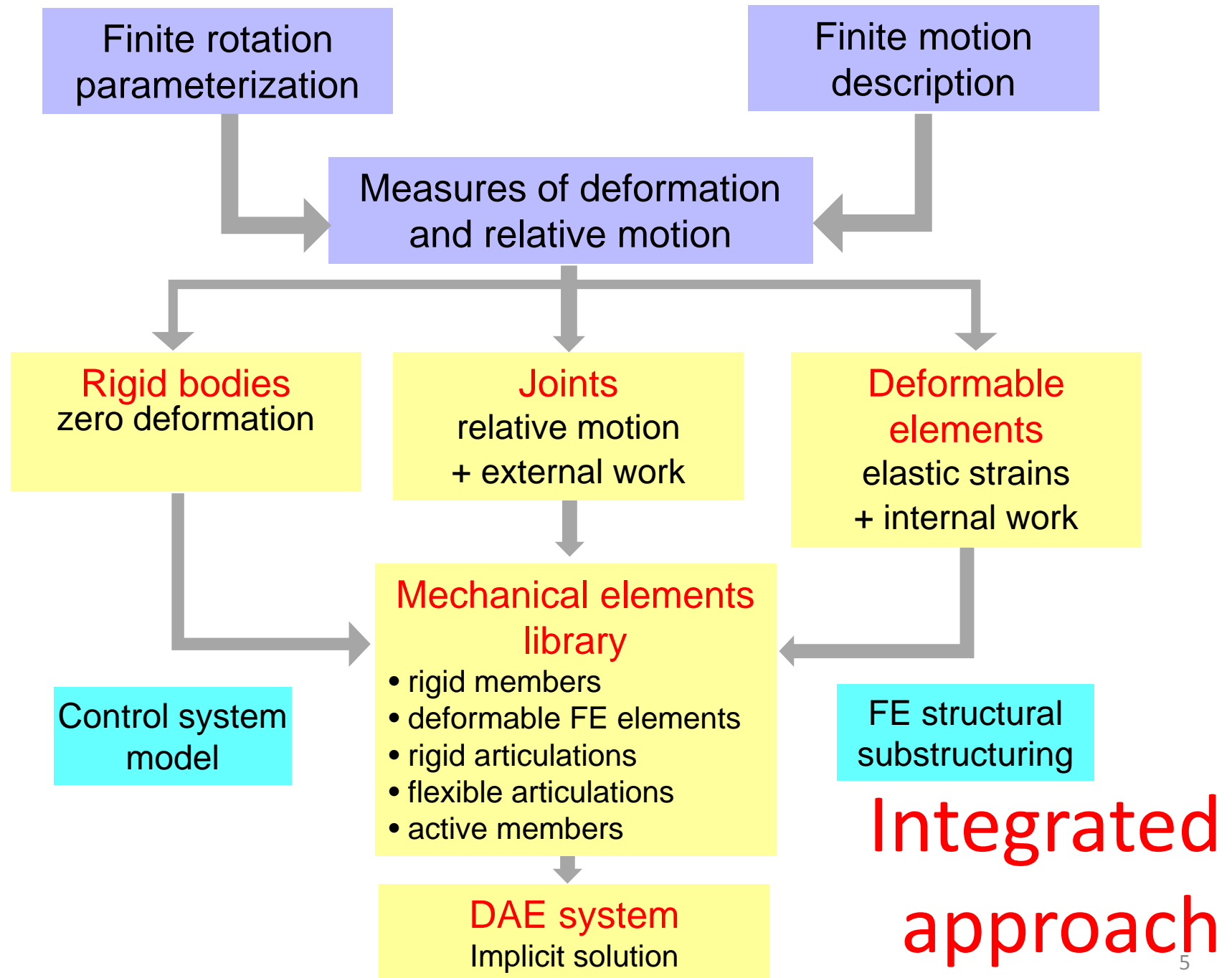
or

Integrated MBS – FE analysis

A long-term trend in simulation?

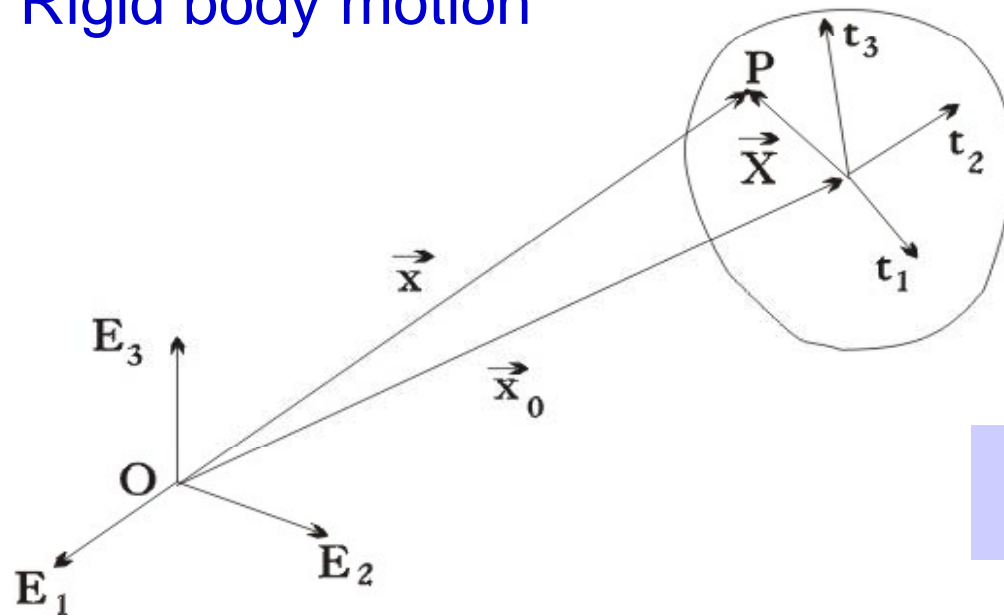
Some steps

- 1983: *Computer Aided Analysis and Optimization of Mechanical System Dynamics*. NATO-ASI, University of Iowa. Organizer: Edward J. Haug.
- 1984: Gérardin M. Finite element approach to kinematic and dynamic analysis of mechanisms using Euler parameters. In International Conference on Numerical Methods for Nonlinear Problems, Barcelona, Spain, 9-13 April 1984.
- 1991: A. Cardona. *An integrated approach to mechanism analysis*. PhD thesis. Université de Liège, Faculté des Sciences Appliquées.
- 2001: Gérardin, M., & Cardona, A. *Flexible multibody dynamics: a finite element approach*. John Wiley.



General kinematics

Rigid body motion



Combination of translation and rotation

$$\mathbf{x}_P = \mathbf{x}_0 + \mathbf{R}\mathbf{X}_P$$

spatial motion
of origin

material
coordinates of
point P

Cartesian position and orientation of point P : are thus uniquely described by

$$(\mathbf{x}_P, \mathbf{R}_P)$$

Rotation parameterization

Orthonormality of R

$$R^T = R^{-1}$$

6 constraints \rightarrow 3 independent parameters

$$\mathbf{a}^T = [\alpha_1 \quad \alpha_2 \quad \alpha_3]$$



$$R = R(\mathbf{a})$$

Possible choices:

- ✓ Euler angles
- ✓ Bryant angles
- ✓ Rodrigues parameters
- ✓ Euler Parameters
- ✓ Cartesian rotation vector
- ✓ Conformal rotation vector
- ✓ ...

Choice criteria:

- ✓ analytical complexity.
- ✓ singular configurations / their handling
- ✓ redundancy (e.g. Euler parameters: 4 \rightarrow 1 constraint) .
- ✓ Composition rule (successive rotations).
- ✓ Differentiation (angular velocities, virtual displacements)
- ✓ Physical meaning

Infinitesimal motion velocity analysis

$$\mathbf{x}_P = \mathbf{x}_0 + \mathbf{R}\mathbf{X}_P$$



infinitesimal
displacements

Infinitesimal
rotations

$$\begin{aligned}\delta \mathbf{x}_P &= \delta \mathbf{x}_0 + \delta \tilde{\boldsymbol{\theta}}(\mathbf{x}_P - \mathbf{x}_0) \\ \mathbf{v}_P &= \mathbf{v}_0 + \tilde{\boldsymbol{\omega}}(\mathbf{x}_P - \mathbf{x}_0)\end{aligned}$$

Linear
velocities

Angular
velocities

with

$$\begin{aligned}\delta \tilde{\boldsymbol{\theta}} &= \delta \mathbf{R}\mathbf{R}^T \\ \tilde{\boldsymbol{\omega}} &= \dot{\mathbf{R}}\mathbf{R}^T\end{aligned}$$

In terms of Cartesian
rotation vector:

$$\begin{aligned}\delta \boldsymbol{\theta} &= \mathbf{T}^T(\boldsymbol{\Psi})\delta \boldsymbol{\Psi} \\ \boldsymbol{\omega} &= \mathbf{T}^T(\boldsymbol{\Psi})\dot{\boldsymbol{\Psi}}\end{aligned}$$

Tangent operator $\mathbf{T}(\boldsymbol{\psi})$:
analytical expression
similar to $\mathbf{R}(\boldsymbol{\psi})$

Kinematics summary

- General description of current point P motion made in Lagrangian form with the following parameters:
 - Absolute position vector x
 - Cartesian rotation vector ψ
- Nonlinear mapping of angular quantities provides *geometrically exact* formalism:

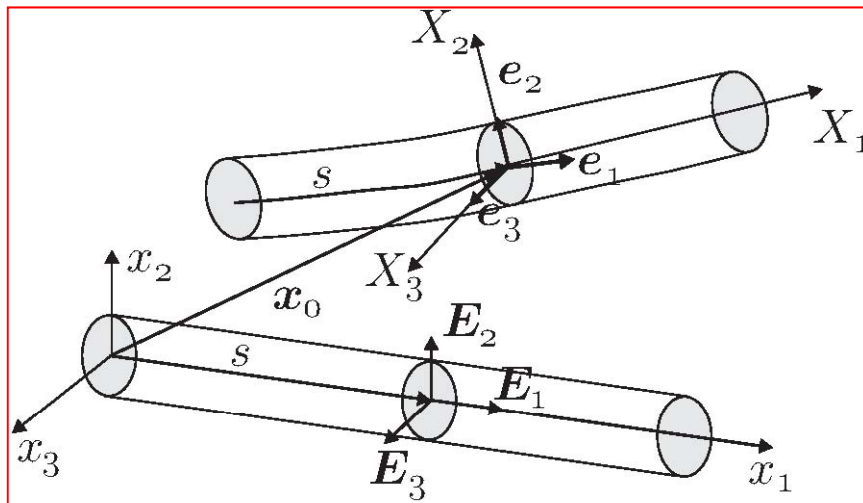
rotations:	$R \leftrightarrow \psi$
angular velocities:	$\omega \leftrightarrow T^T(\Psi)\dot{\Psi}$
angular variations:	$\delta\theta \leftrightarrow T^T(\Psi)\delta\Psi$

- Same formalism is applied to any MBS component (rigid bodies, joints, nonlinear 1D/2D/3D deformable members, superelements, subassemblies)
- Updated Lagrangian description of rotations is generally adopted.

Example: «geometrically exact» beam

Kinematic assumptions

- Beam is initially straight
- Cross sections remain plane and do not deform
- Shear deformation of neutral axis allowed
- Rotational energy of cross sections taken into account



Strains

Stress-strain relationships

Local equilibrium

Virtual work expression

Strain measures

Obtained from position gradients along s before and after deformation

$$D(s, X_2, X_3) = \mathbf{R}^T \frac{d\mathbf{x}}{ds} - \frac{d\mathbf{X}}{ds} \rightarrow \underbrace{\mathbf{R}^T \left(\frac{d\mathbf{x}_0}{ds} - \mathbf{e}_1 \right)}_{\text{Neutral axis}} + \underbrace{\mathbf{R}^T \frac{d\mathbf{R}}{ds} \mathbf{Y}}_{\text{Cross section}}$$

Deformation of neutral axis

$$\Gamma(s) = \mathbf{R}^T \left(\frac{d\mathbf{x}_0}{ds} - \mathbf{e}_1 \right)$$

$$\Gamma_1 = \mathbf{e}_1^T \frac{d\mathbf{x}_0}{ds} - 1 \quad \text{Extension of neutral axis}$$

$$\Gamma_i = \mathbf{e}_i^T \frac{d\mathbf{x}_0}{ds} \quad (i = 2, 3) \quad \text{Shear strains}$$

Measure of curvature

$$\tilde{\mathbf{K}} = \mathbf{R}^T \frac{d\mathbf{R}}{ds} \quad \text{Curvature matrix}$$

$$\mathbf{K} = \mathbf{T}(\Psi) \frac{d\Psi}{ds} \quad \text{Curvature vector}$$

Material measures

$$\mathbf{D} = \Gamma - \tilde{\mathbf{Y}} \mathbf{K}$$

K_1 torsion of neutral axis
 K_2, K_3 bending curvatures

Elastic 4-bar mechanism



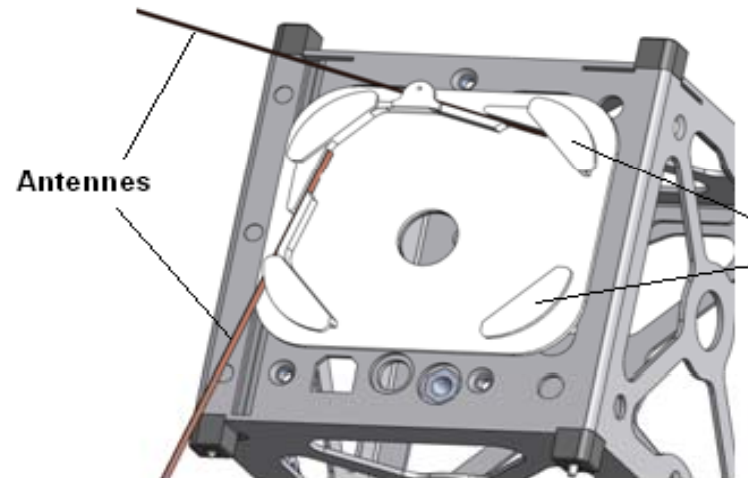
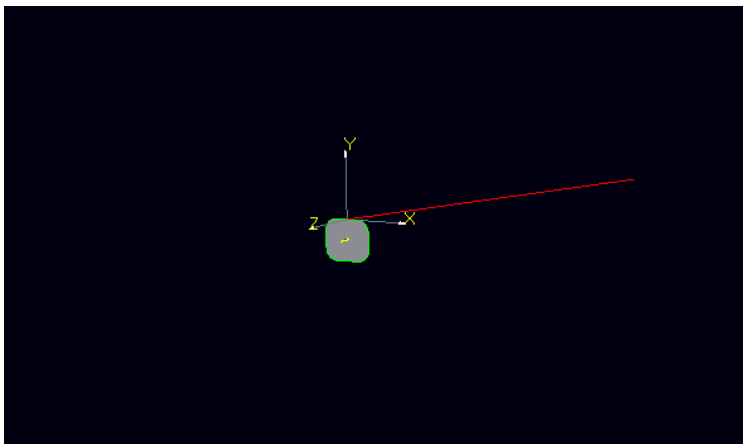
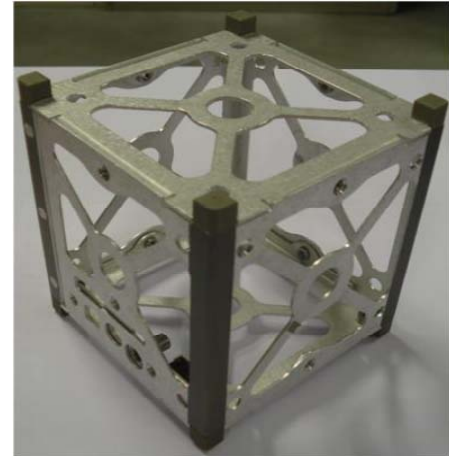
offset

elastic rocker

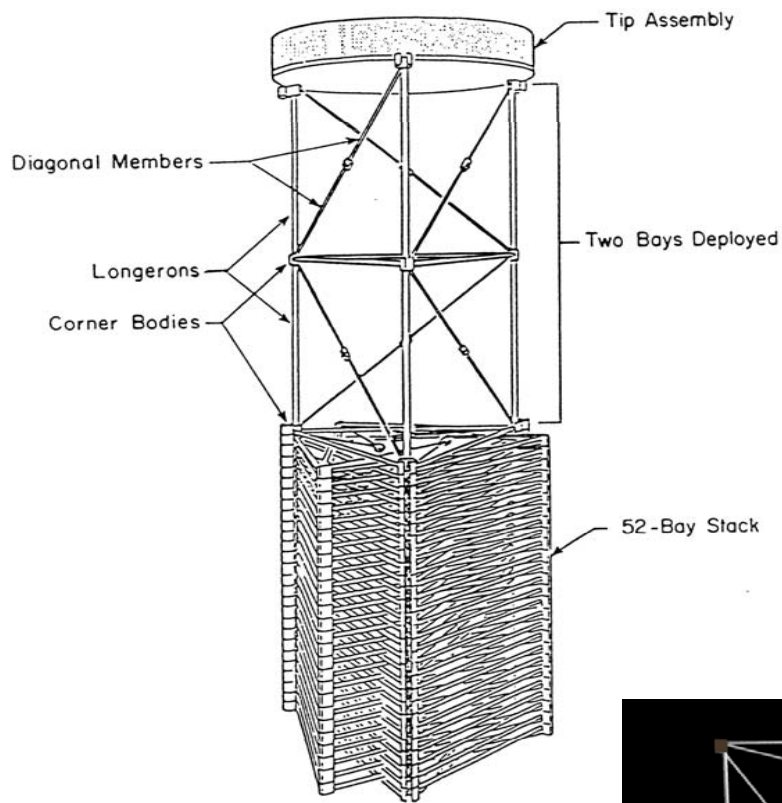
clamped

OUFTI-1 satellite

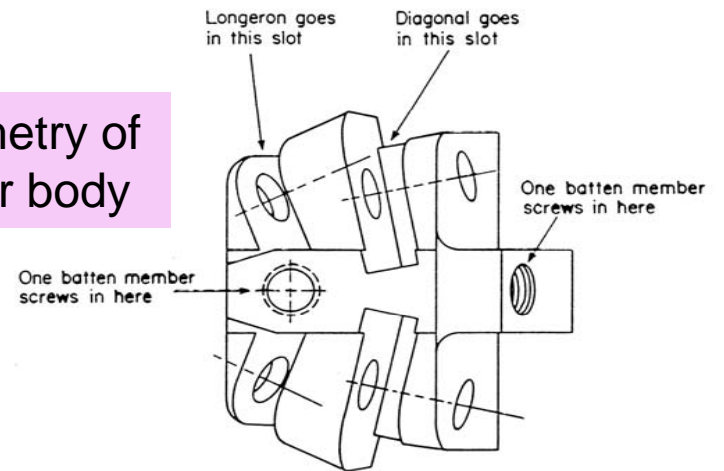
- Student CubeSat designed in Liège
- 10x10x10 cm
- 1 kg
- D-STAR amateur-radio
- digital-communication protocol
- Two deployable antennas



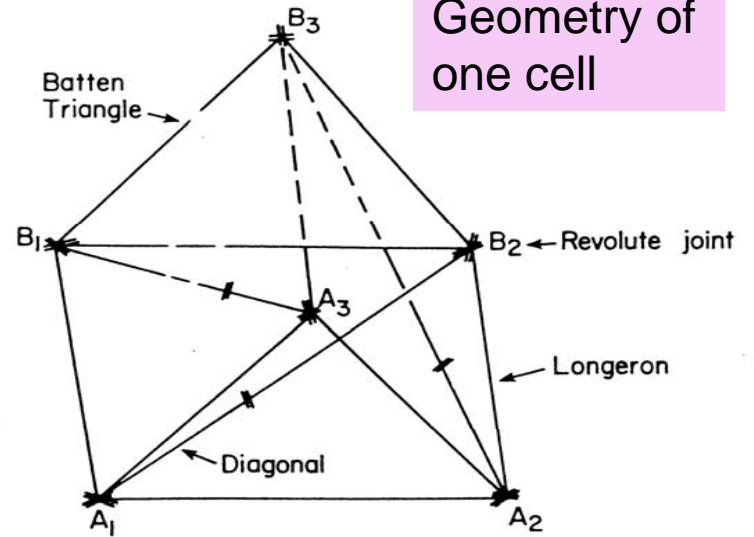
Deployment of astromast cell



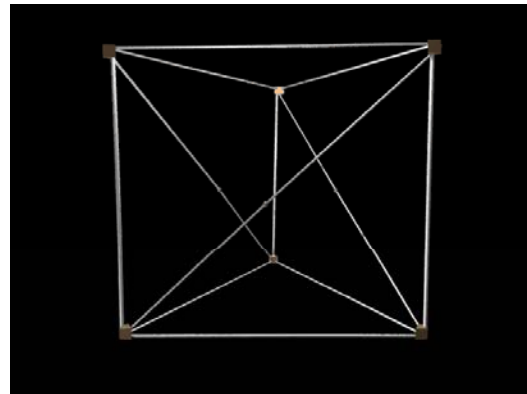
Geometry of corner body



Geometry of one cell



Stacking method: 2 bays deployed

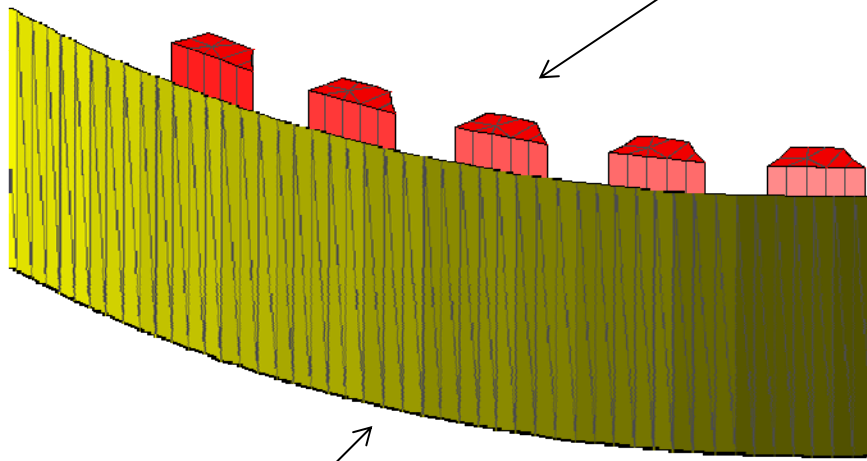


Modeling of transmission belt

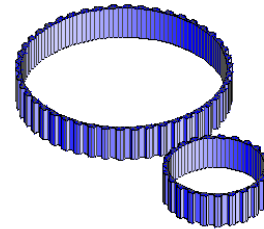
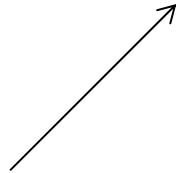
Structural hypotheses

Belt: rubber

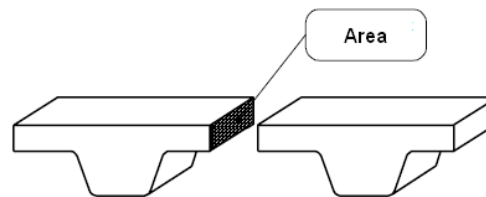
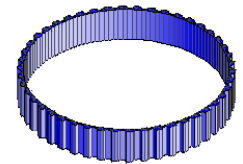
Volume elements



Membrane elements

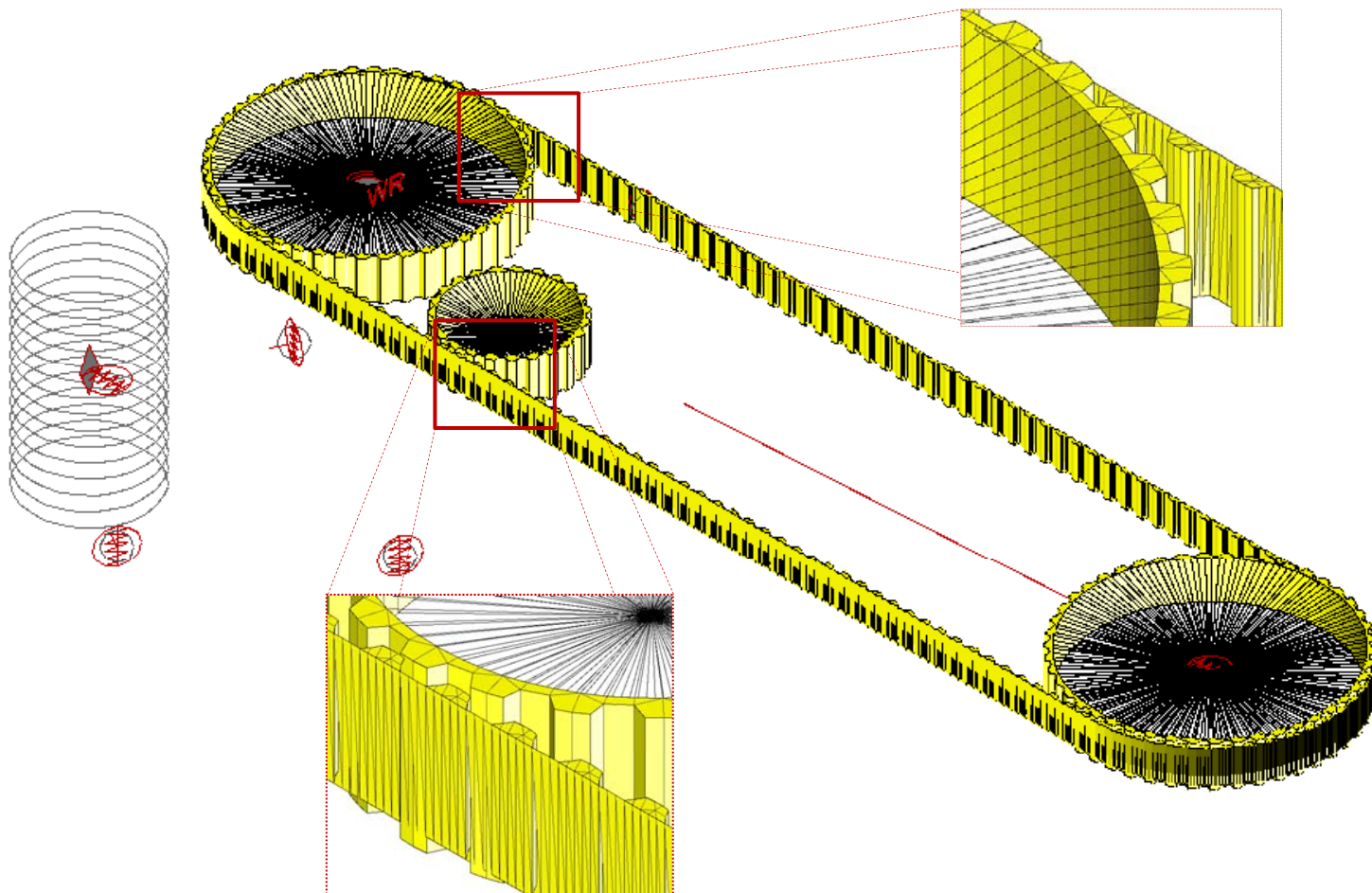


Pulleys and sprocket: steel

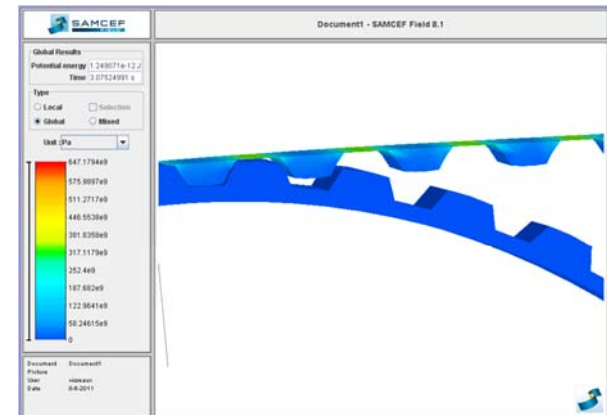
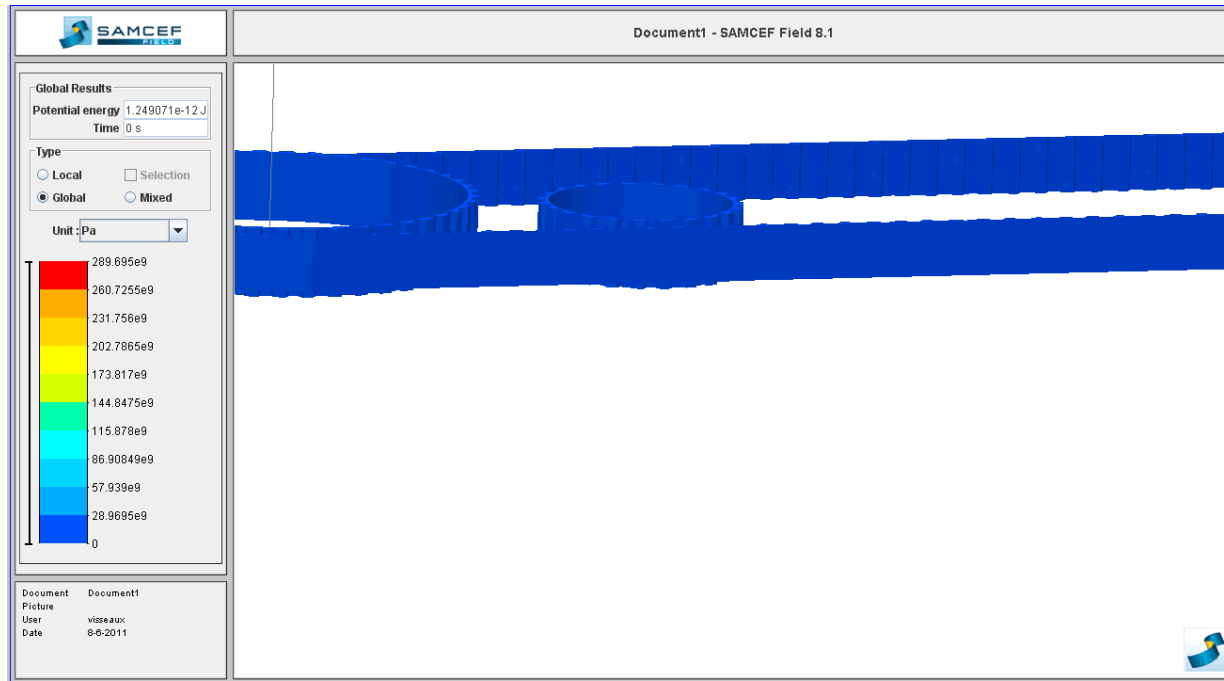


Modelling of transmission belt

- Finite element mesh: 7500 nodes, 14600 elements.



Dynamics of transmission belt



General formulation

Variational approach

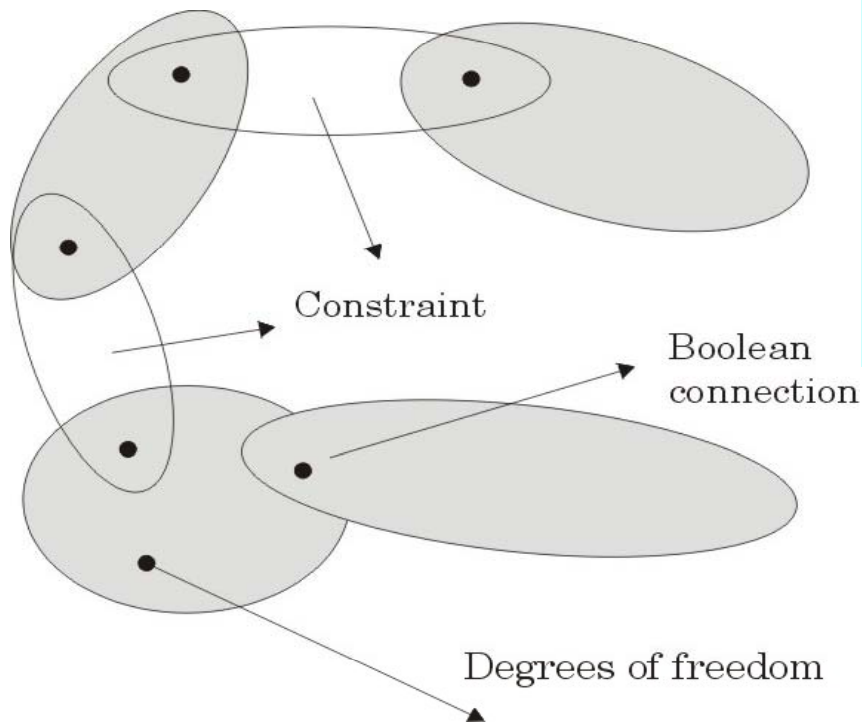
$$\delta \int_{t_1}^{t_2} \left(\mathcal{K} - \mathcal{W} - \mathcal{P} - k\lambda^T \Phi - \frac{p}{2} \Phi^T \Phi \right) dt = \mathbf{f}_{nc}^T \delta \mathbf{q}$$

- \mathbf{q} Generalized coordinates.
- $\mathcal{K}(\mathbf{q}, \dot{\mathbf{q}})$ Kinetic energy.
- $\mathcal{W}(\mathbf{q})$ Strain energy.
- $\mathcal{P}(\mathbf{q})$ Potential energy of external loads.
- $\Phi(\mathbf{q}, t)$ Kinematic constraints.
- λ Lagrange multipliers.
- \mathbf{f}_{nc} Non-conservative forces.
- p Penalty coefficient.
- k Scaling coefficient.

Summation
over
elements

Augmented Lagrangian
method with scaling →
improved robustness of
linear solution

System assembly



\mathbf{q} = DOF at structural level

\mathbf{q}_e = DOF at element level

\mathbf{L}_e = DOF localization operator(boolean)

λ = lagrangian multipliers

- Boolean constraints: localization of DOF
- Implicit constraints: algebraic treatment

$$\mathbf{q}_e = \mathbf{L}_e \mathbf{q}$$

$$\Phi(\mathbf{q}_e, \dot{\mathbf{q}}_e, t) = 0$$

System topology results implicitly from Boolean assembly and constraint description

Dynamic equilibrium

- Formulation using the Augmented Lagrangian method

$$\begin{cases} \mathbf{M}\ddot{\mathbf{q}} + \mathbf{B}^T(k\boldsymbol{\lambda} + p\boldsymbol{\Phi}) = \mathbf{g}(\mathbf{q}, \dot{\mathbf{q}}, t) \\ p\boldsymbol{\Phi}(\mathbf{q}, t) = 0 \end{cases}$$

- \mathbf{M} constant with respect to translation DOF.
 - Exact treatment of constraints
 - Well-conditioned iteration matrix
- Implicit / iterative Solution \rightarrow recast in residual form

$$\begin{cases} \mathbf{r}(\mathbf{q}, \dot{\mathbf{q}}, \ddot{\mathbf{q}}, \boldsymbol{\lambda}) = \mathbf{g}(\mathbf{q}, \dot{\mathbf{q}}, t) - \mathbf{M}\ddot{\mathbf{q}} - \mathbf{B}^T(k\boldsymbol{\lambda} + p\boldsymbol{\Phi}) = 0 \\ p\boldsymbol{\Phi}(\mathbf{q}, t) = 0 \end{cases}$$

Implicit time integration Newmark type methods

- One-step methods → obey to the general form

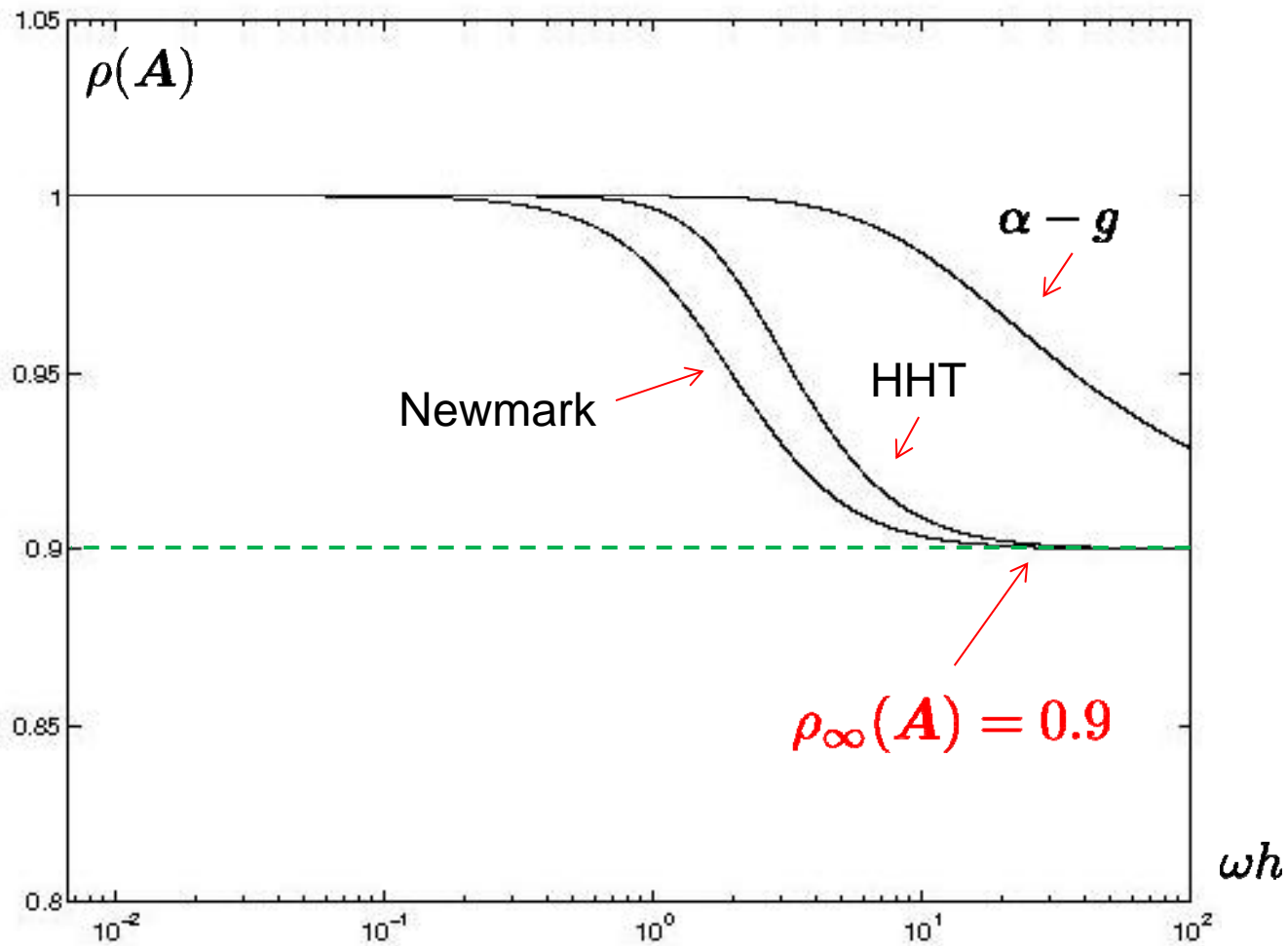
$$\begin{bmatrix} \mathbf{q}_{n+1} \\ \dot{\mathbf{q}}_{n+1} \\ \ddot{\mathbf{q}}_{n+1} \end{bmatrix} = \mathbf{A} \begin{bmatrix} \mathbf{q}_n \\ \dot{\mathbf{q}}_n \\ \ddot{\mathbf{q}}_n \end{bmatrix}$$

- Can provide *unconditional stability over entire frequency range*.
- Accuracy /stability properties adjusted through free parameters.
 - Second-order accuracy can be achieved.
 - Stability: governed by *spectral radius* = highest eigenvalue of amplification matrix \mathbf{A} .

$$\rho(\mathbf{A}) \leq 1$$

(Guarantees stability of index-3 DAE system).

Spectral radius of Newmark type methods



Modified α - g method

- Newmark interpolation of displacements and velocities

$$\begin{aligned}\dot{\mathbf{q}}_{n+1} &\simeq \dot{\mathbf{q}}_n + (1 - \gamma)h\mathbf{a}_n + \gamma h\mathbf{a}_{n+1} \\ \mathbf{q}_{n+1} &\simeq \mathbf{q}_n + h\dot{\mathbf{q}}_n + \left(\frac{1}{2} - \beta\right)h^2\mathbf{a}_n + \beta h^2\mathbf{a}_{n+1}\end{aligned}$$

- Pseudo-accelerations \mathbf{a}_n defined through collocation

$$(1 - \alpha_m)\mathbf{a}_{n+1} + \alpha_m\mathbf{a}_n = (1 - \alpha_f)\ddot{\mathbf{q}}_{n+1} + \alpha_f\ddot{\mathbf{q}}_n$$

- Residual form of equilibrium

$$\begin{cases} \mathbf{r}(\mathbf{q}_{n+1}, \dot{\mathbf{q}}_{n+1}, \ddot{\mathbf{q}}_{n+1}, \boldsymbol{\lambda}) = 0 \\ \Phi(\mathbf{q}_{n+1}, t_{n+1}) = 0 \end{cases}$$

$$\rightarrow \begin{cases} \mathbf{r}(\mathbf{q}_{n+1}, \boldsymbol{\lambda}) = 0 \\ \Phi(\mathbf{q}_{n+1}) = 0 \end{cases}$$

- 4 parameters $(\beta, \gamma, \alpha_f, \alpha_m)$

Nonlinear system to be solved iteratively

Equilibrium iteration

- Linear solution step

$$\begin{bmatrix} \mathbf{S} & k\mathbf{B}^T \\ k\mathbf{B} & 0 \end{bmatrix} \begin{bmatrix} d\mathbf{q} \\ d\lambda \end{bmatrix} = \begin{bmatrix} \mathbf{r}(\mathbf{q}^*, \lambda^*) \\ -k\Phi(\mathbf{q}^*) \end{bmatrix}$$

with matrix \mathbf{S} linear combination (coefficients depending upon integration scheme) of matrices

$$\mathbf{M}, \frac{\partial \mathbf{g}}{\partial \mathbf{q}}, \frac{\partial \mathbf{g}}{\partial \dot{\mathbf{q}}}, p\mathbf{B}\mathbf{B}^T + \frac{\partial \mathbf{B}^T}{\partial \mathbf{q}}(k\lambda + p\Phi)$$

- *Sparsity linked to FE mesh topology.*
- Can be solved using standard linear solver for large sparse systems.
- The λ can be assimilated to ordinary DOF

$$\mathbf{S}d\mathbf{q} = \mathbf{r}(\mathbf{q}^*)$$

Time step size control

- Drawbacks due to use of predefined, fixed time step size:
 - Time step too large: higher frequencies filtered out → loss of detail in the response.
 - Time step too small: increase of computer time, waste of resources.
- Time step adjustment during numerical integration can be based on a measure of integration error computed from

$$e = \left(\beta - \frac{1}{6} \right) h^2 \Delta \ddot{\mathbf{q}}$$

- Adequate strategy should:
 - Avoid exceeding prescribed tolerance.
 - Keep time step fixed for sufficiently long periods.

Joint modeling

Level 1: *functional description*

- purely kinematic model
- description by algebraic constraints
- rigid behavior
- « perfect » interaction

Level 2: *macroscopic engineering description*

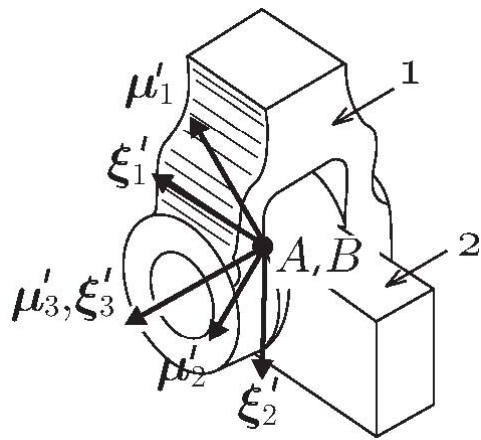
- semi-rigid behavior
- partial description by algebraic constraints.
- Addition of global constitutive laws (e.g. compliance, friction).

Level 3: *detailed / mesoscopic description*

- 3D geometric representation
- Account of structural detailing
- Finite element modeling

Revolute joint: functional description

Parts A and B

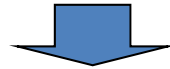


2 rotation constraints

$$\mu'_1{}^T \xi'_3 = 0 \quad \text{and} \quad \mu'_2{}^T \xi'_3 = 0$$

$$\Phi_1 = \mu_1^T R_A^T R_B \xi_3 = 0$$

$$\Phi_2 = \mu_2^T R_A^T R_B \xi_3 = 0$$



$$\delta\Phi = B\delta q$$

3 position constraints

$$\mathbf{x}_B = \mathbf{x}_A$$

Boolean

$$B = \left[\frac{\partial \Phi_i}{\partial q_j} \right]$$

$$\{\mu'_1, \mu'_2, \mu'_3\}$$

$$\{\xi'_1, \xi'_2, \xi'_3\}$$

$$\mu'_i = R_A \mu_i$$

$$\xi'_i = R_B \xi_i$$

→ Base vectors of body A - reference configuration

→ Base vectors of body B - reference configuration

→ Base vectors of body A - current configuration

→ Base vectors of body B - current configuration

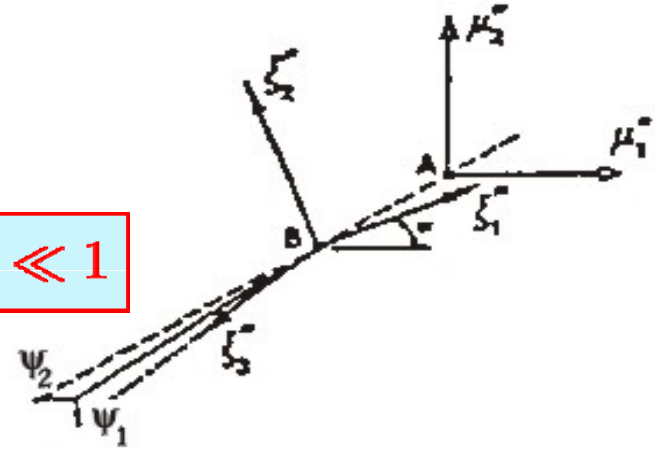
Revolute joint: level 2 description

angular deformations

$$\begin{aligned} \mu_1'^T \xi_3' &= \sin \psi_2 \simeq \psi_2 \\ \mu_2'^T \xi_3' &= -\sin \psi_1 \simeq -\psi_1 \end{aligned}$$

translation deformations

$$\mathbf{u} = \mathbf{R}_A^T (\mathbf{x}_B - \mathbf{x}_A) \quad \|\mathbf{u}\| \ll 1$$



Strain energy

$$\mathcal{W} = \frac{1}{2} \mathbf{u}^T \mathbf{H}_u \mathbf{u} + \frac{1}{2} \boldsymbol{\psi}^T \mathbf{H}_\psi \boldsymbol{\psi}$$

elastic coefficients

Internal forces



Tangent stiffness

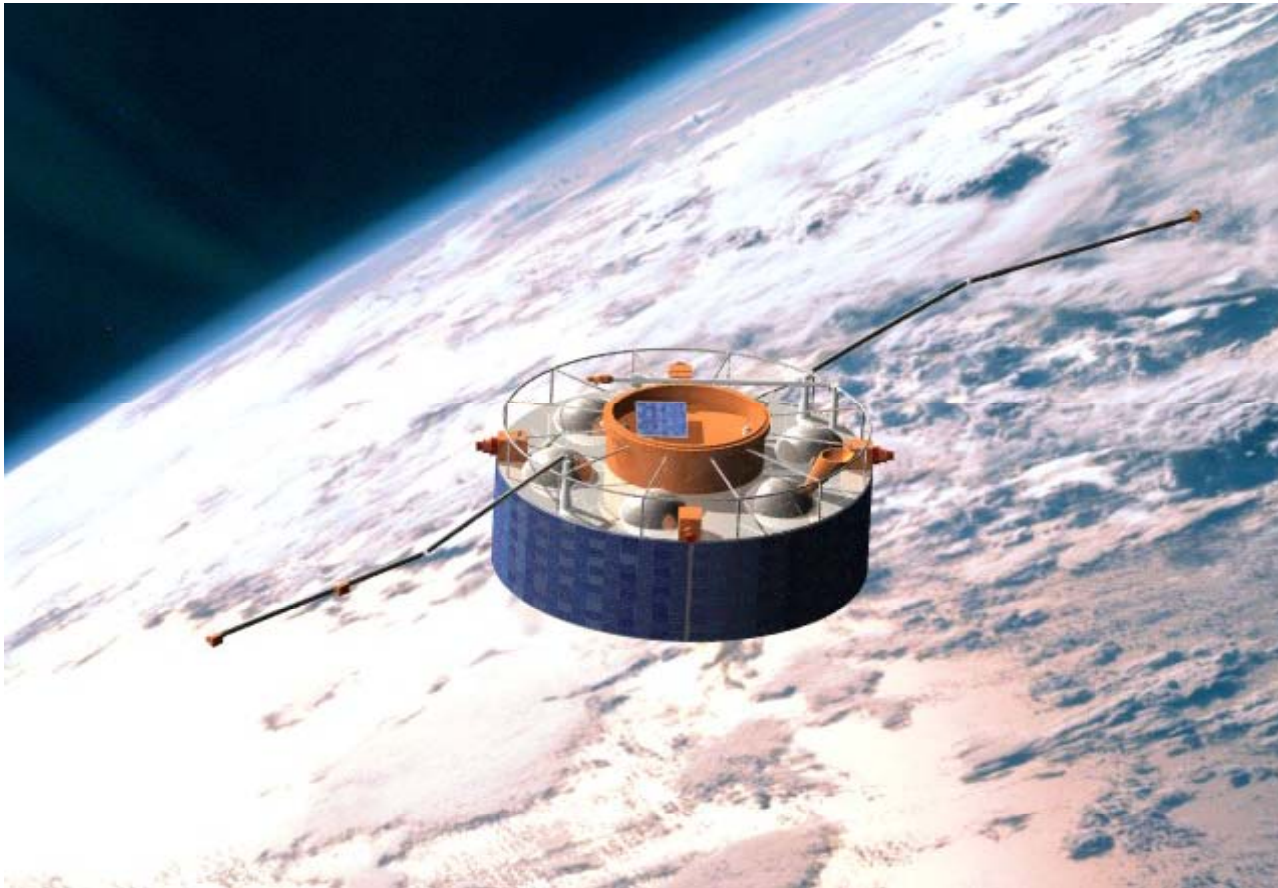
$$\mathbf{g}_{int} = -\frac{\partial \mathcal{W}}{\partial \mathbf{q}_j}$$

Specialized hinges for deployment of space structures

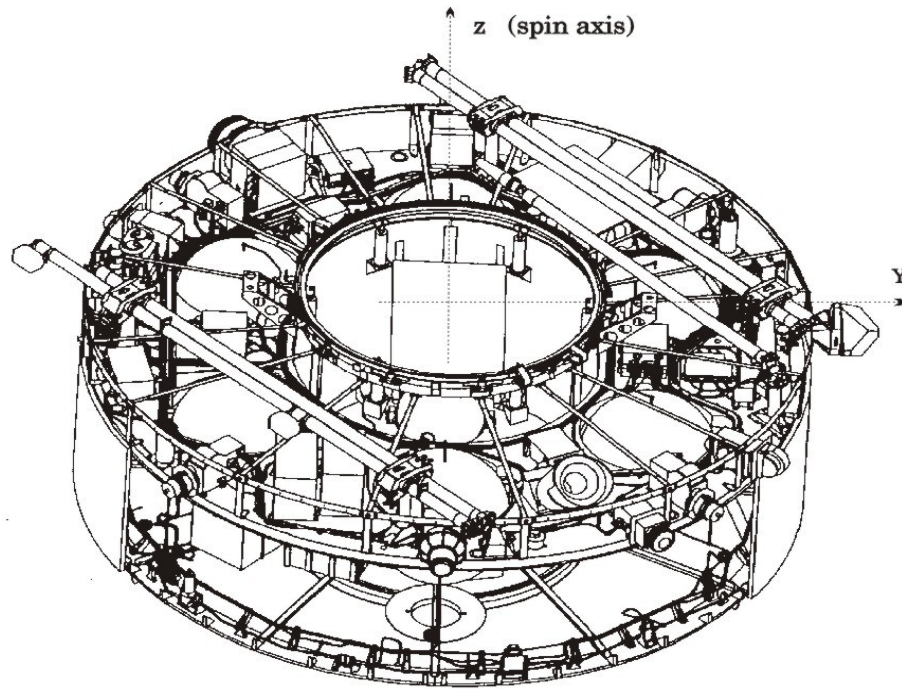
Desirable characteristics

- Passive motorization (energy release)
 - Adequate torque / rotation relationship.
 - Auto-locking.
- High transverse stiffness
- High precision motion → minimum backlash and friction
- High stiffness in folded and locked configurations.
- Minimum size.
- Well-characterized stiffness and damping properties.

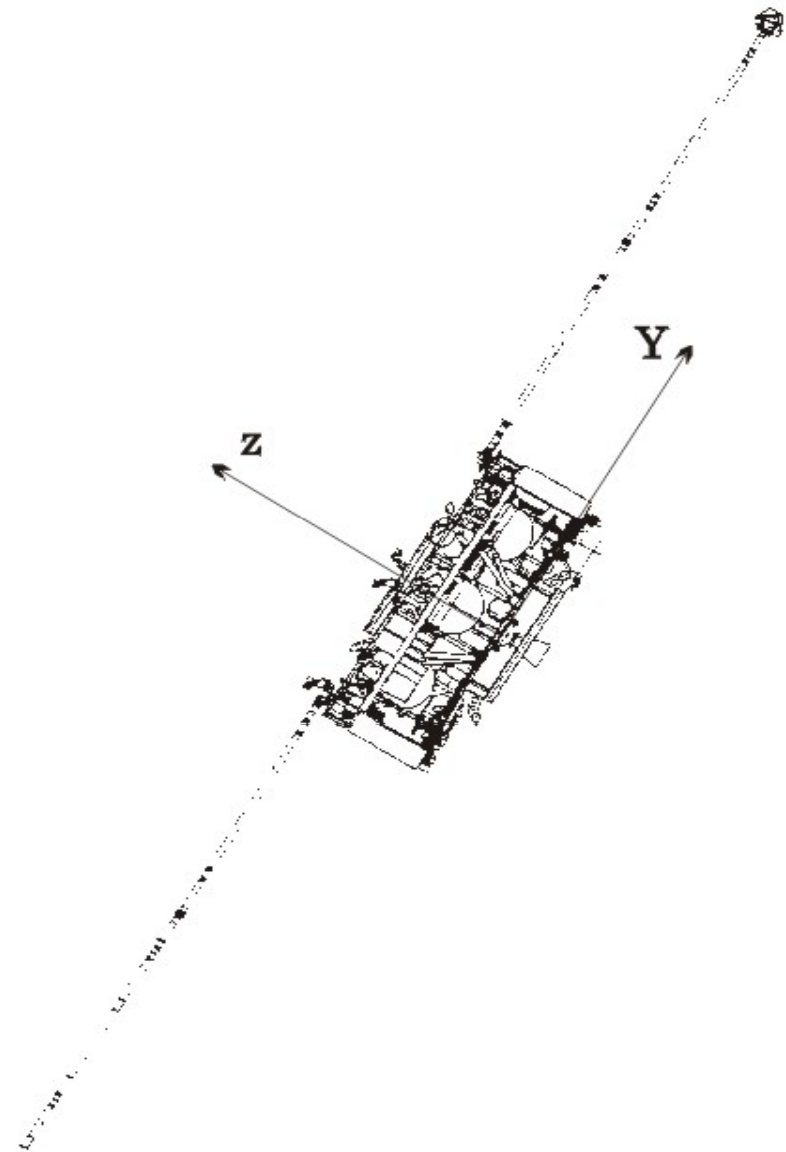
Simulation of Cluster satellite boom deployment



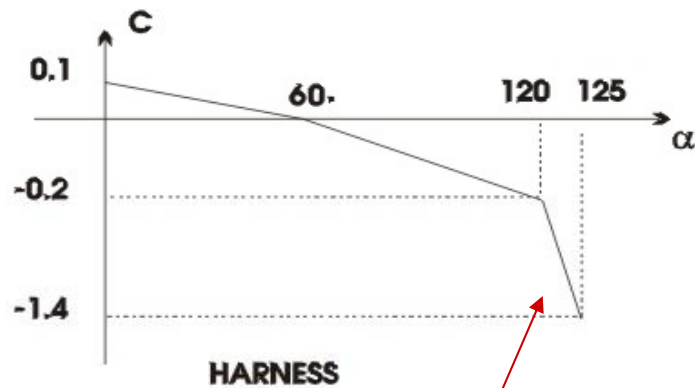
Boom design



- 2 folded booms
- spring actuators
- harnesses



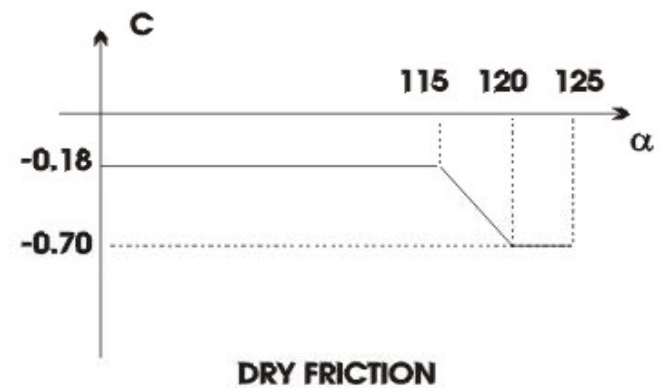
Motorized hinge characteristics



HARNESS

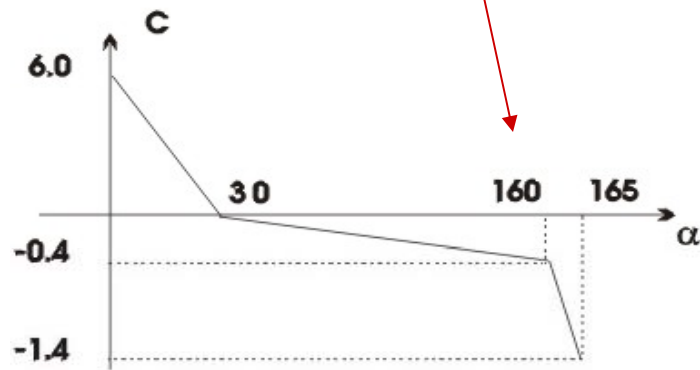
INNER HINGE

Locking characteristics



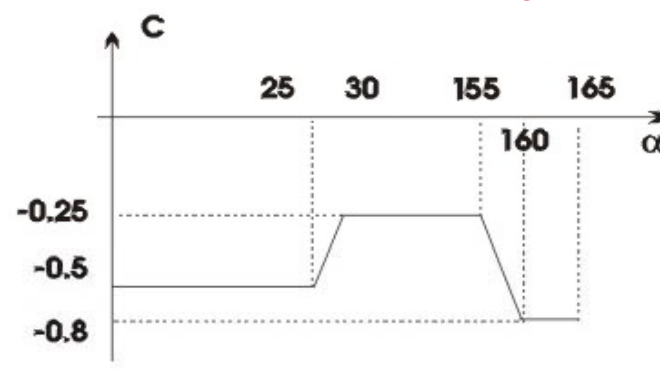
DRY FRICTION

Introduced through regularization



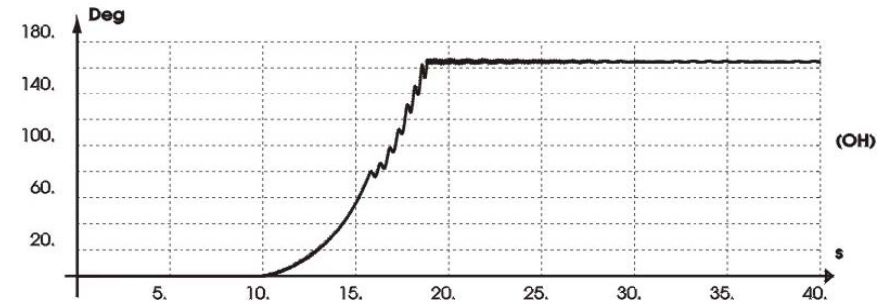
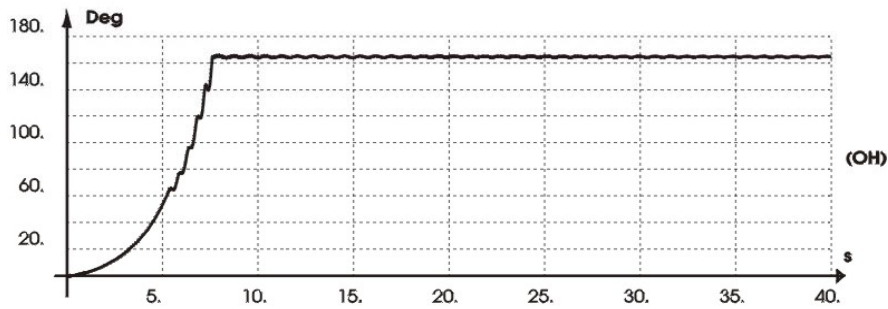
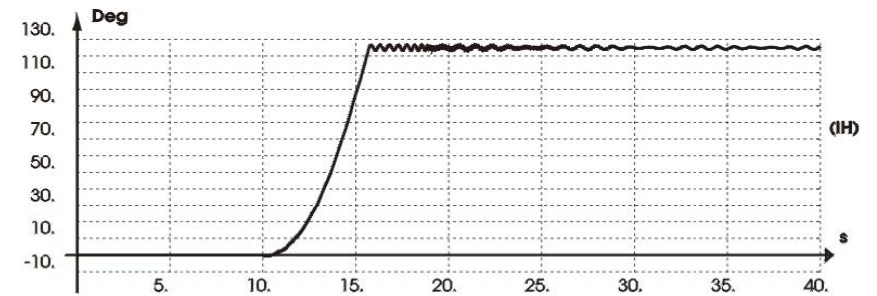
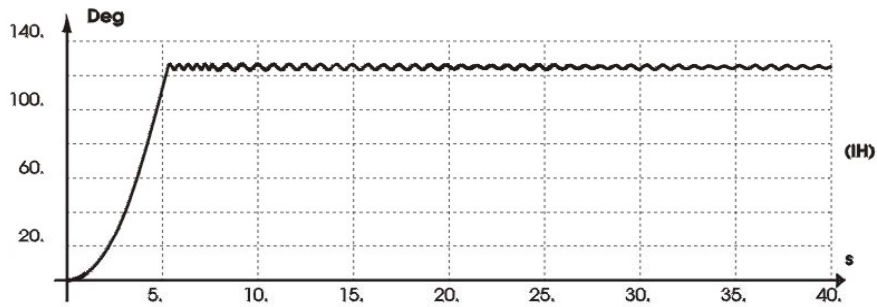
HARNESS

OUTER HINGE



DRY FRICTION

Deployment with flexible booms

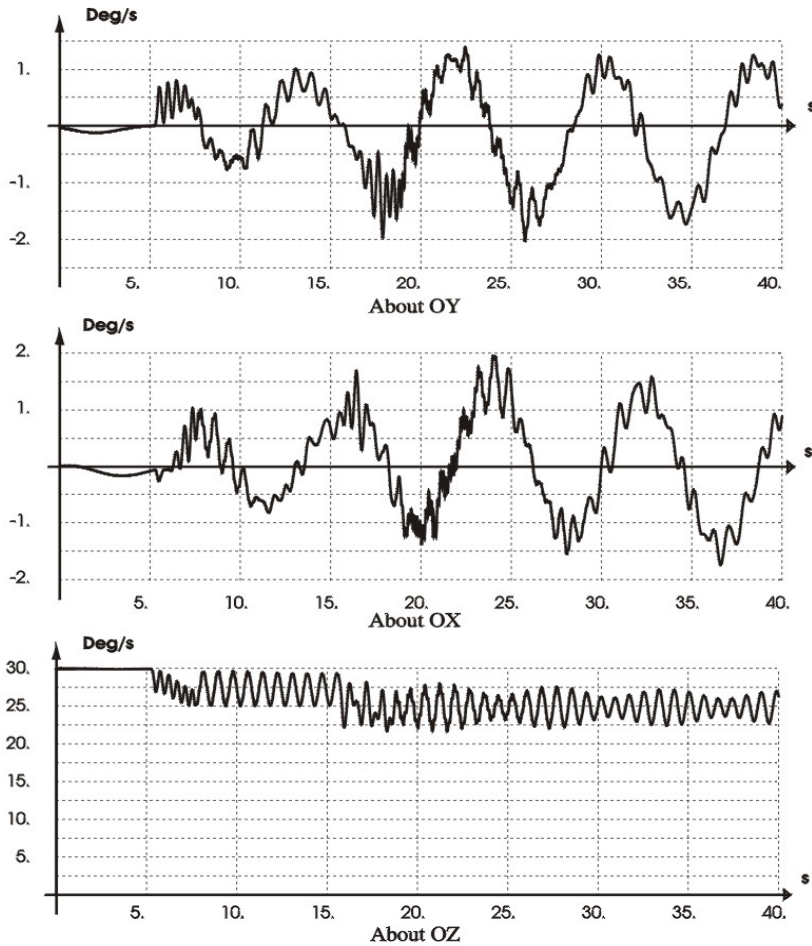


Boom -Y

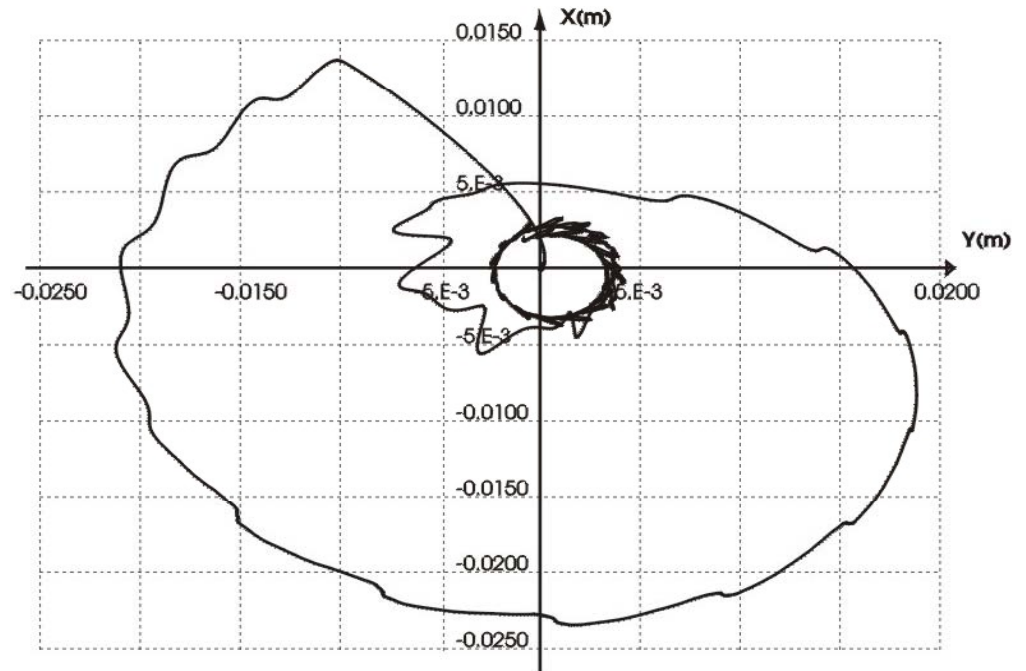
Boom +Y

Angular displacements

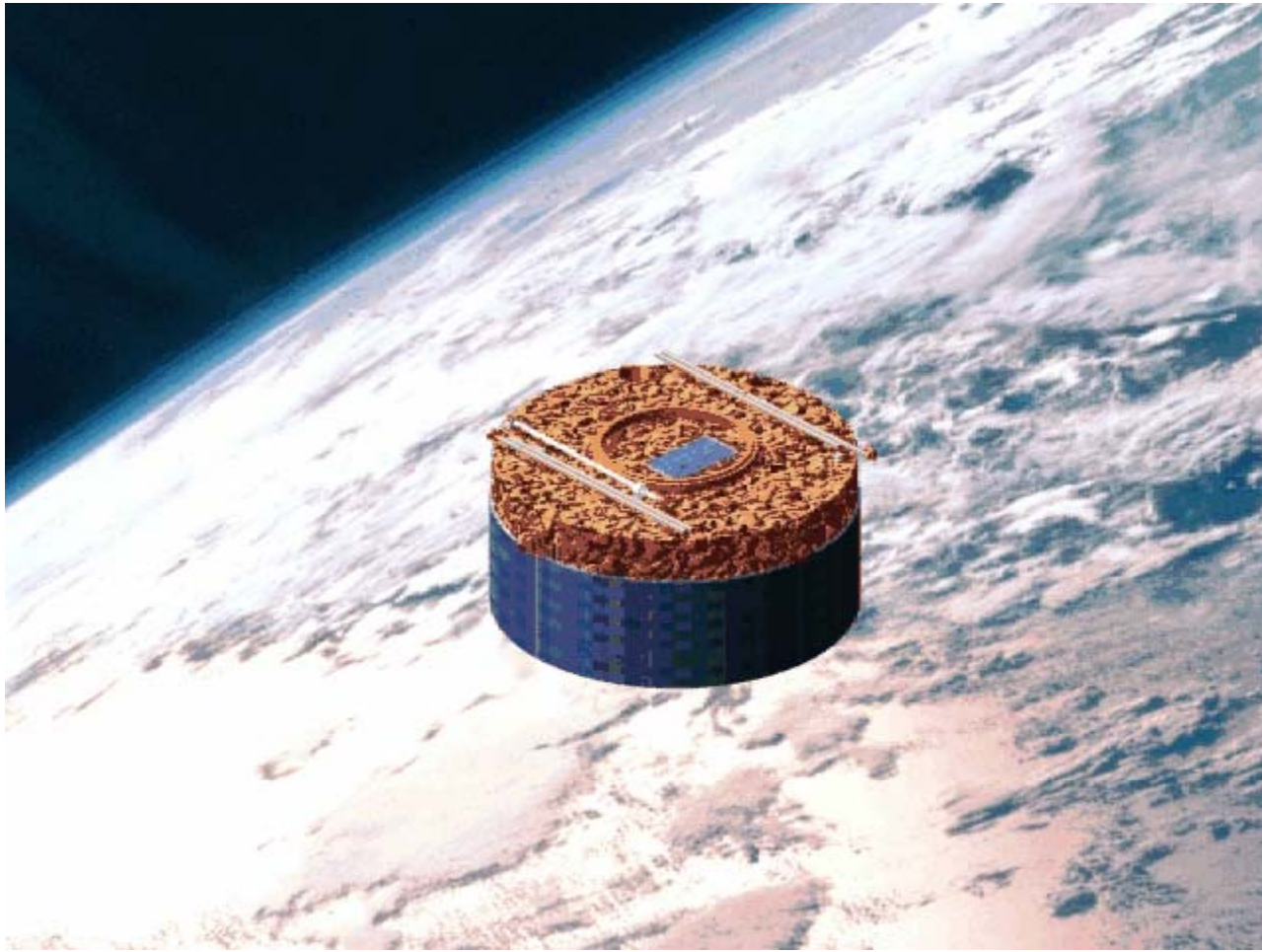
Deployment with flexible booms



Angular velocity of CM



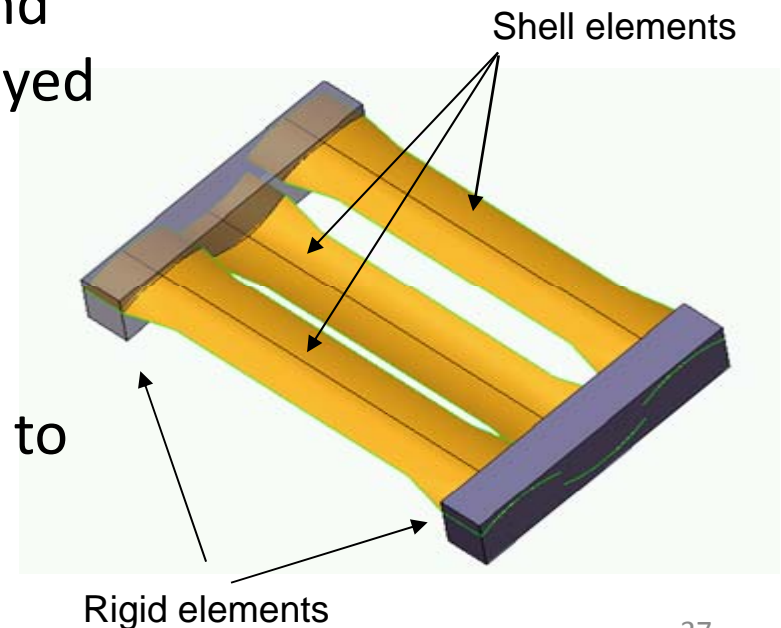
Trajectory of CM



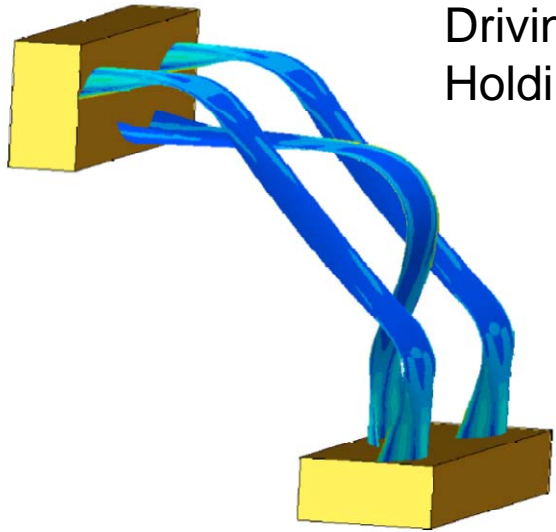
Mesoscopic joint modeling: MAEVA hinge

- Improved version of Carpentier joint (patented design).
- Consists of three steel strips with curved cross section.
- Combines guidance (due to anisotropic stiffness), actuation (spring effect) and locking (high holding torque in deployed configuration).
- Minimization of mechanical parts.
- No sliding / moving interfaces.
- But: detailed 3D modeling essential to represent non-linear behavior and buckling phenomena.

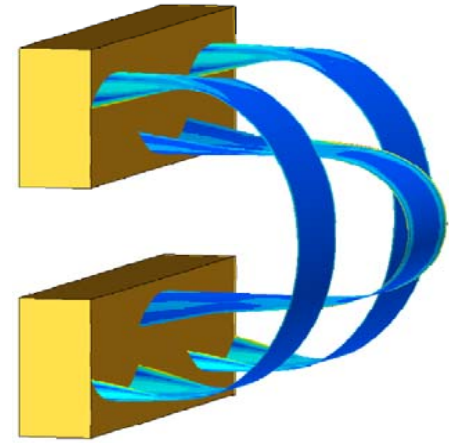
- Sicre, J. et al. Application of MAEVA hinge to Myriade microsatellite deployment needs. *ESMATS* 2005.
- Lathuiliere M. et al. Deployment of appendices using MAEVA hinges: progress in dynamic models. *ESMATS* 2009.



Static behavior



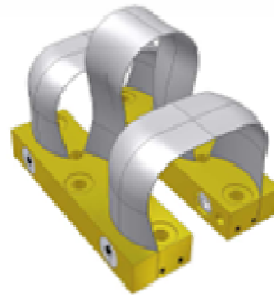
Driving torque : 0.152 Nm
Holding torque : 6.67 Nm



Driving torque : 0.194 Nm
Holding torque : 6.67 Nm

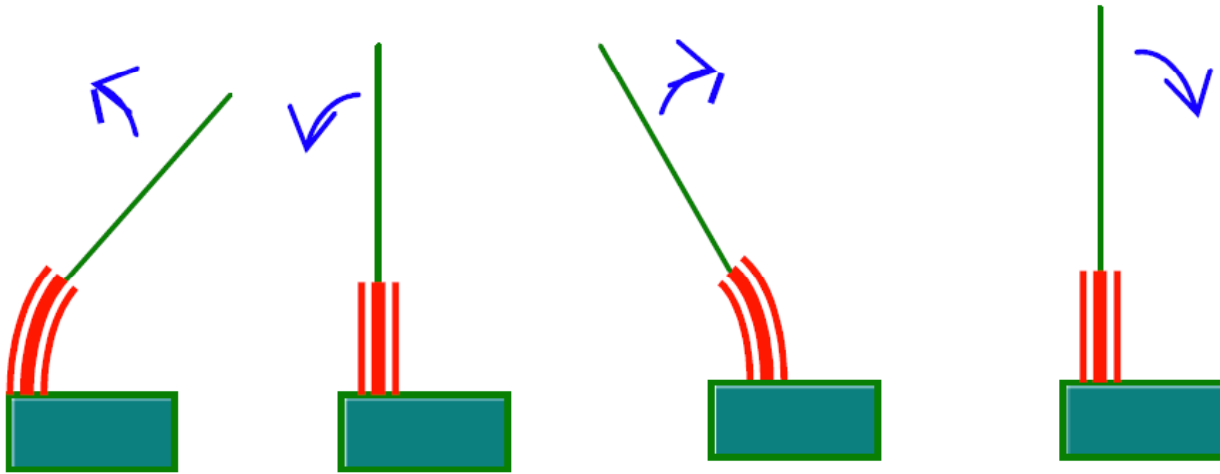


Deployed configuration



Stowed configurations

Features of dynamic behavior

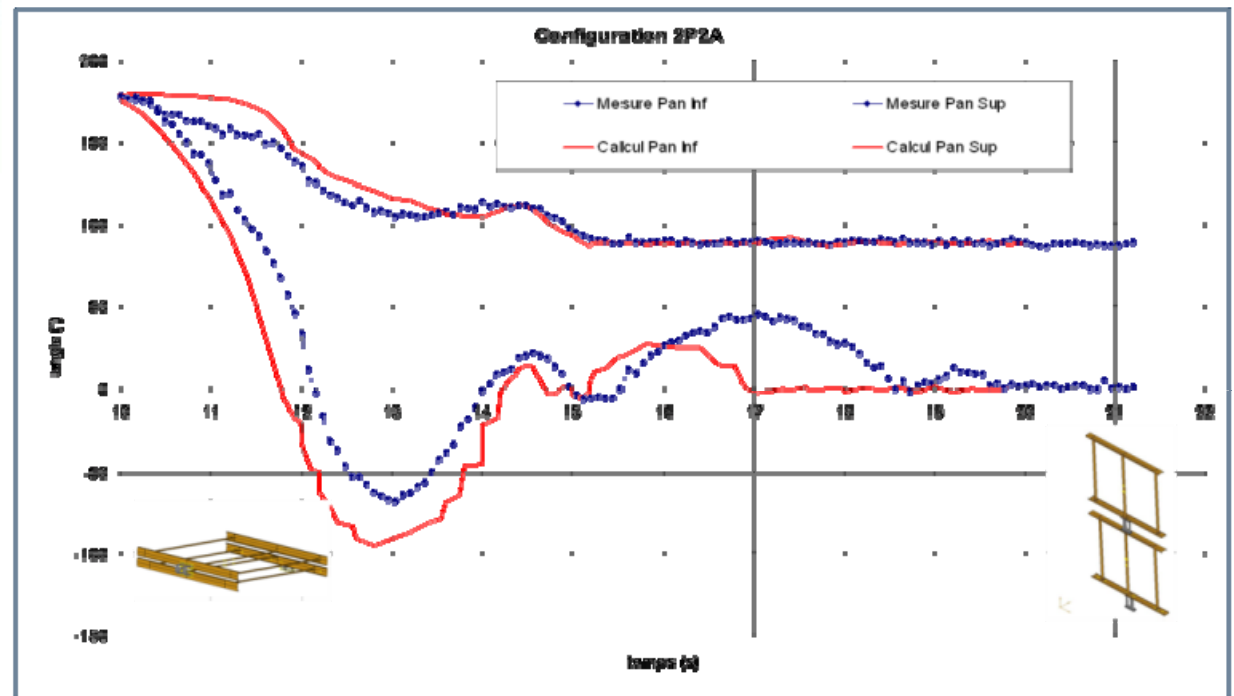
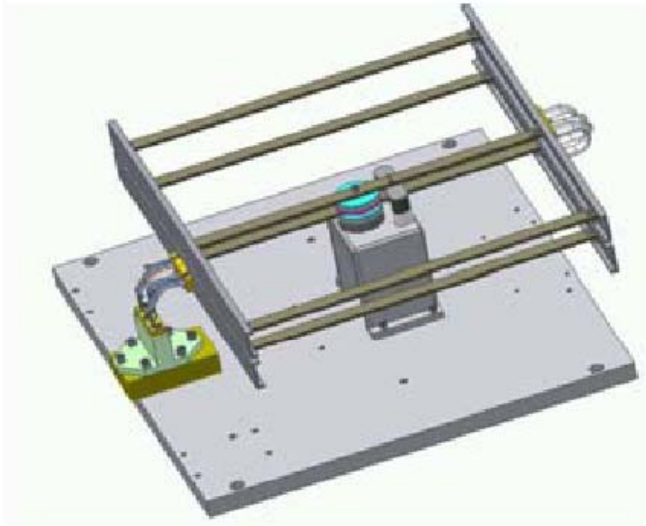


1. Oscillations around equilibrium position

2. Low torsional stiffness



2-panel deployment



Modal synthesis in multibody dynamics

Goal

- To represent complex structural members by standard, linear FE models

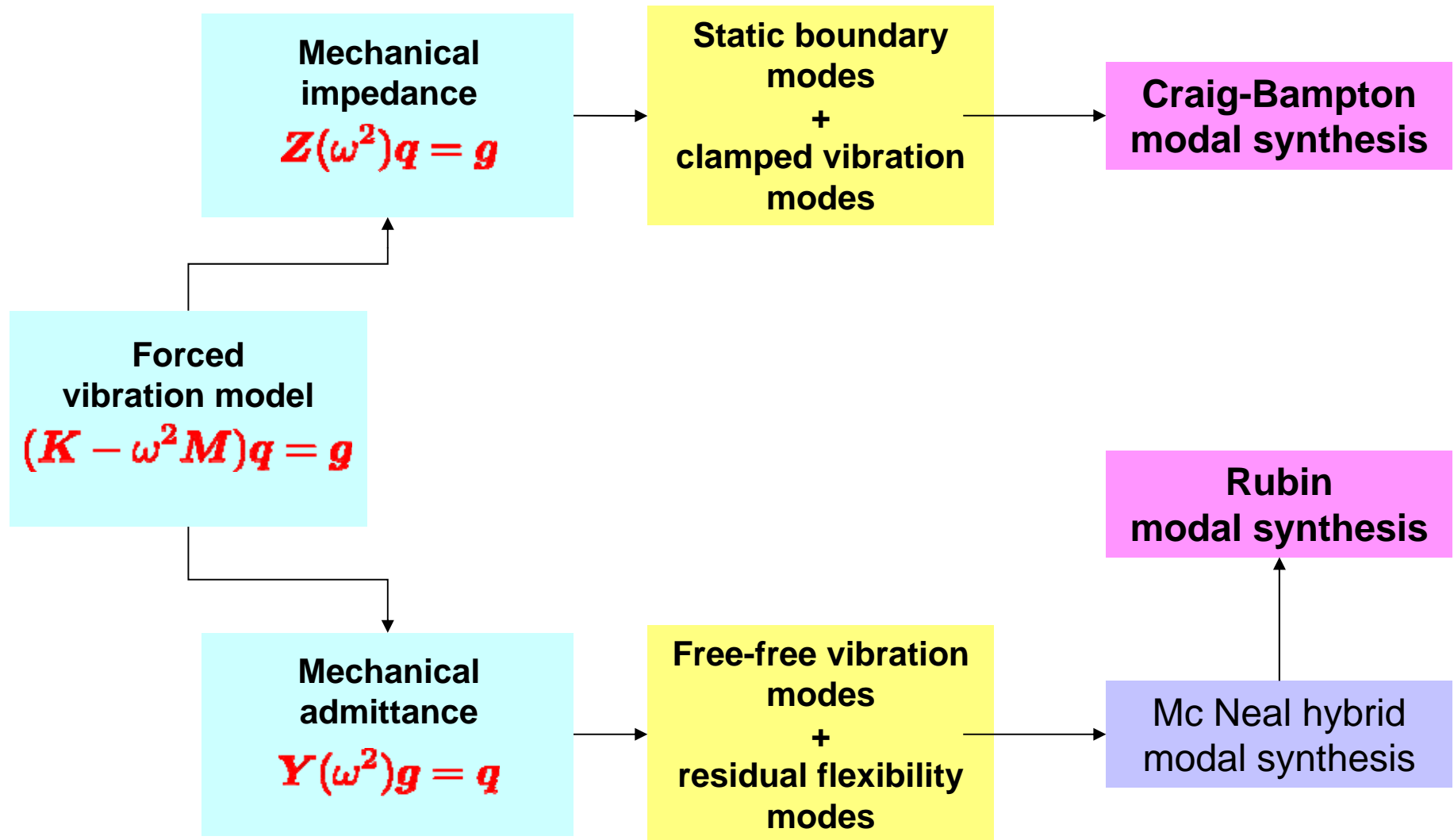
Method

- Assume linear behavior in local (**co-rotational**) frame
- Produce reduced model with
 - u attachment modes to external system
 - u reduced set of internal modes to represent local behavior

Limitations

- Due to linearity assumption
- Recuperation of model components (**superelement**) from standard linear analysis → missing information on inertia.

Modal synthesis: dual approaches



Underlying kinematic assumption

$$\mathbf{x} = \mathbf{x}_0 + \mathbf{R}_0(\mathbf{X} + \mathbf{u})$$

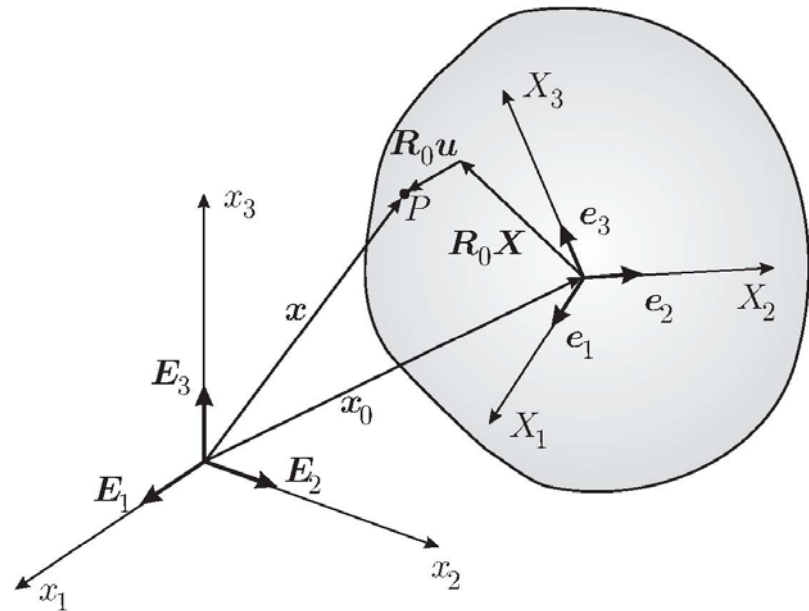
$$\Psi = \Psi_0 \circ \psi$$

- Solve with respect to elastic displacements

$$\begin{bmatrix} \mathbf{u} \\ \psi \end{bmatrix} = \begin{bmatrix} \mathbf{R}_0^T (\mathbf{x} - \mathbf{x}_0) - \mathbf{X} \\ (-\Psi_0) \circ \Psi \end{bmatrix}$$

- Modal representation of elastic displacements

$$\begin{bmatrix} \mathbf{u} \\ \psi \end{bmatrix} = \bar{\Phi} \mathbf{y}$$



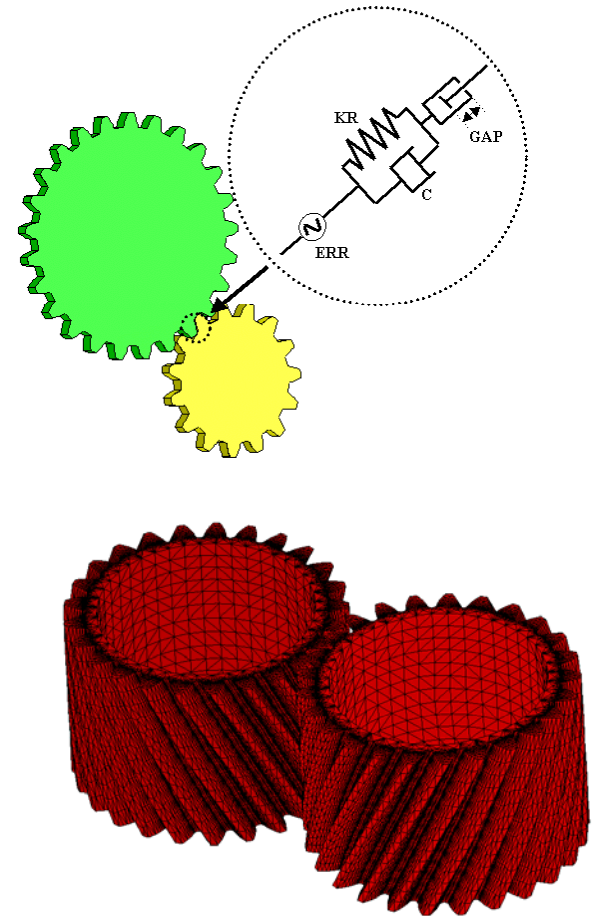
- Small displacement assumption in local frame

$$\frac{\|\mathbf{u}\|}{\|\mathbf{X}\|}, \|\psi\| \ll 1$$



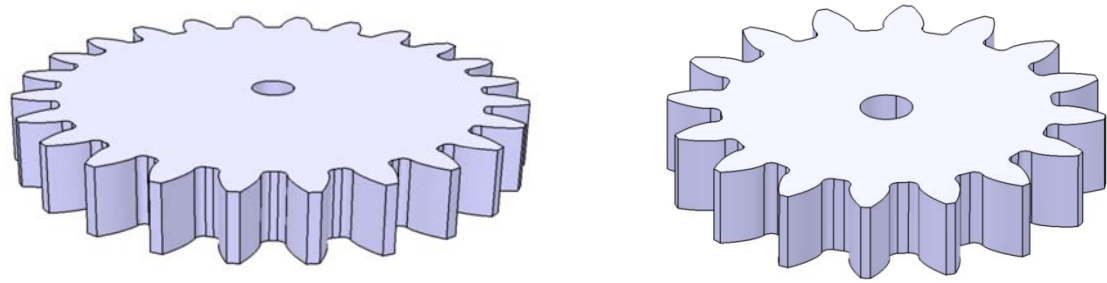
Application example: Gear modeling

- ❑ **Macroscopic gear models** [Cardona, 1995]
 - Kinematic constraints between wheel centers.
 - Gear wheels = rigid bodies.
 - Spring-damper along normal pressure line.
 - Crude /empirical modeling of meshing defaults: (e.g. backlash, friction, load transmission error).
- ❑ **Contact condition between full FE models**
 - Gear teeth deformation and gear web accurately taken into account.
 - Meshing defaults naturally modeled.
 - Long simulation times → limited use.
- ❑ **Contact condition between superelements**
 - Gear wheel flexible behavior globally accounted for.
 - Determination of actual contact points by means of 3D gear wheel geometry.
 - Study of misalignment, backlash, gear hammering,...

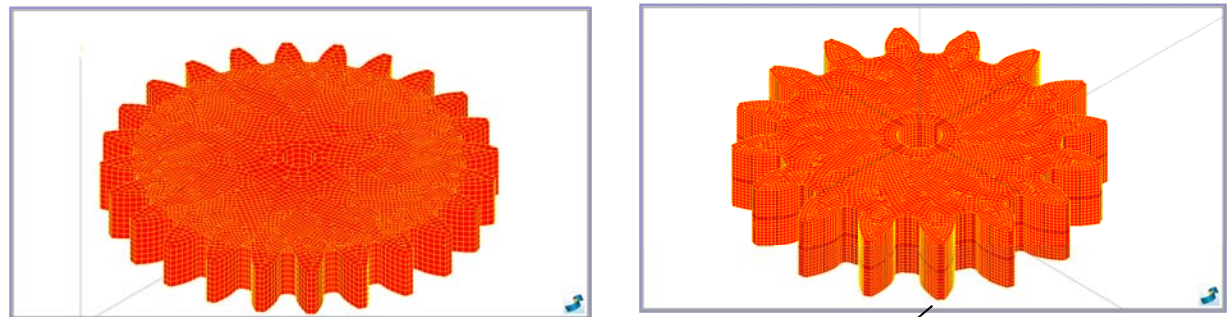


Simple gear system

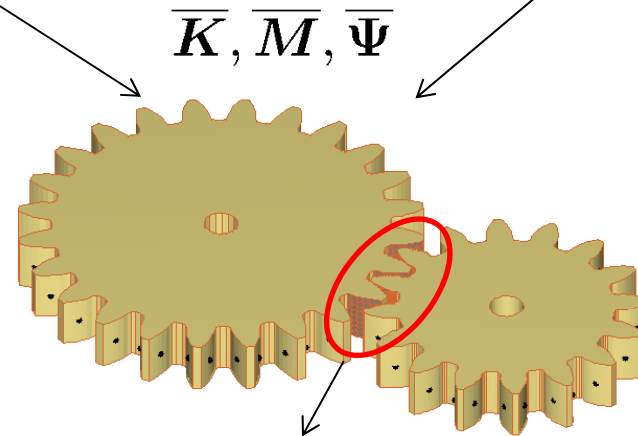
1) CAD modeling



2) FE modeling and model reduction



3) Simulation of unilateral contact between superelements (MATLAB)



Selection strategy of slave-master flank pairs

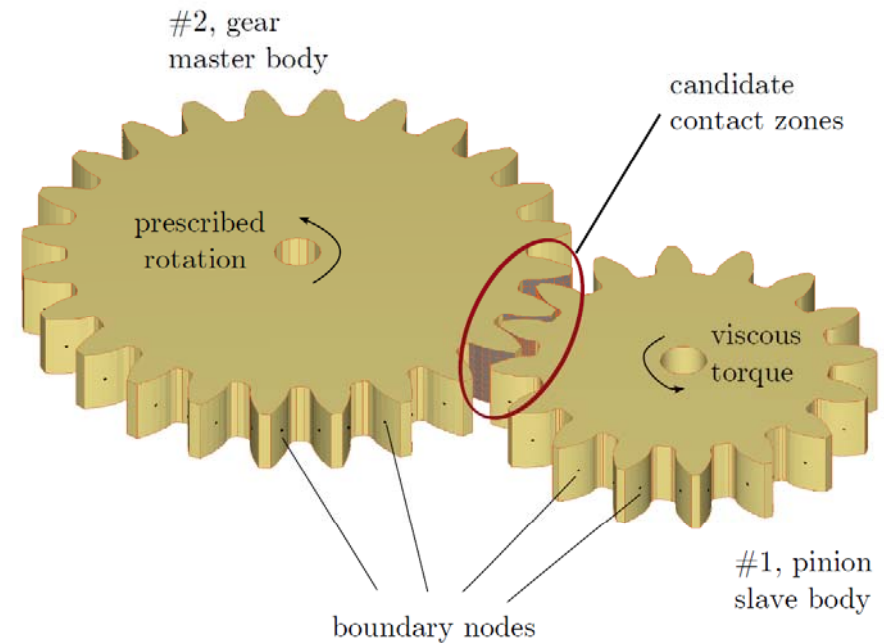
Simple gear system simulation

Craig & Bampton modal synthesis

	pinion	gear
Number of teeth [-]	16	24
Pitch diameter [mm]	73,2	109,8
Outside diameter [mm]	82,64	118,64
Root diameter [mm]	62,5	98,37
Addendum coef. [-]	0,196	0,125
Tooth width [mm]		15
Pressure angle [deg]		20
Module [mm]		4,5

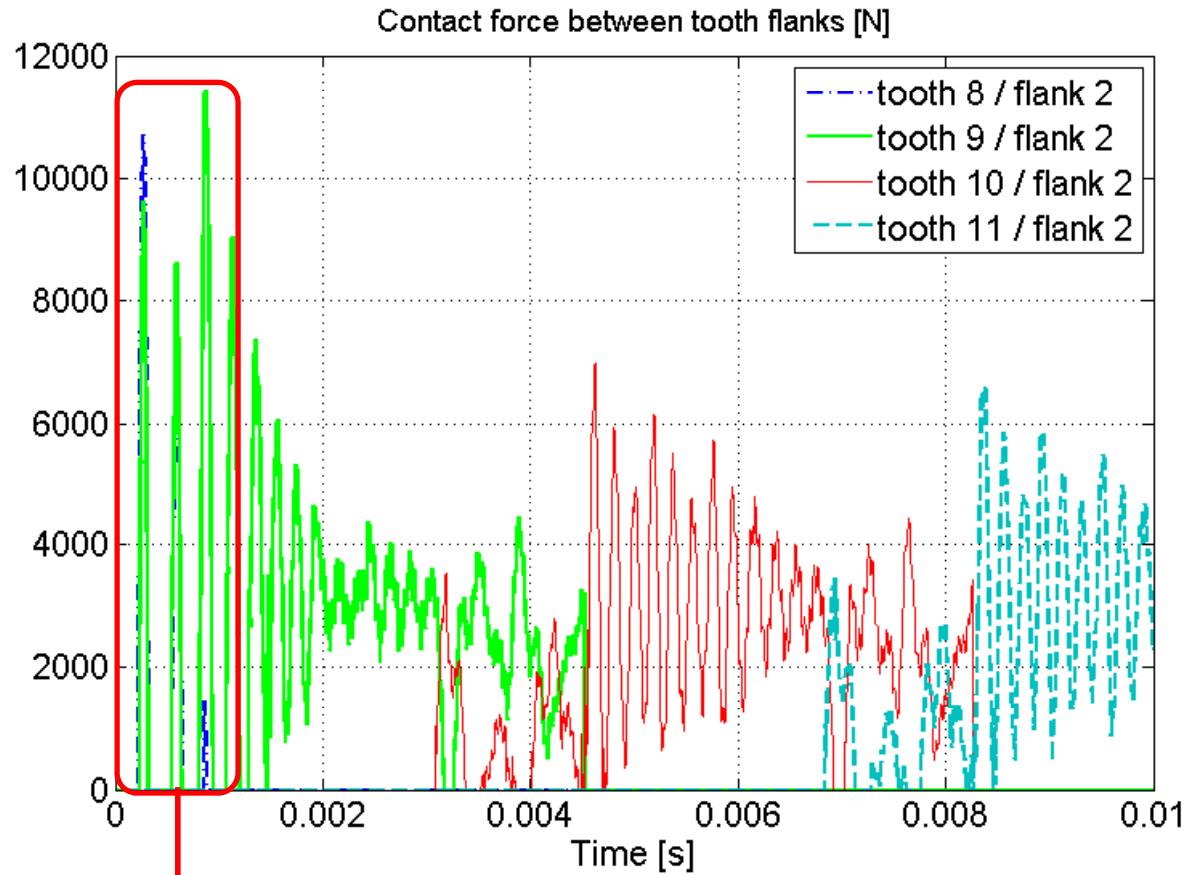
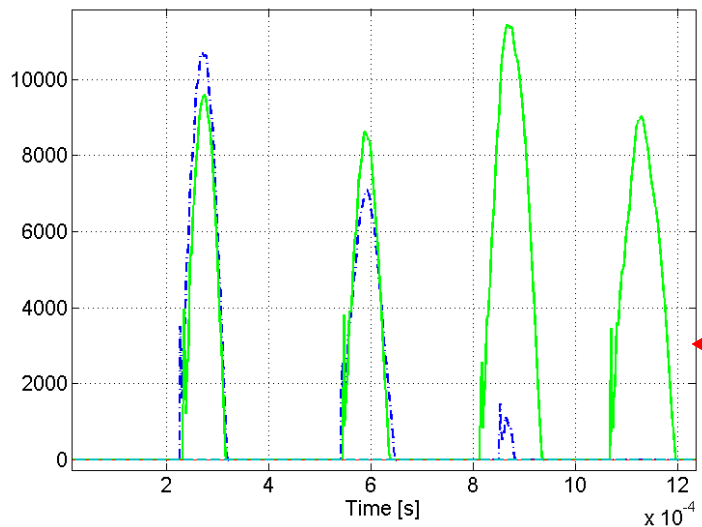
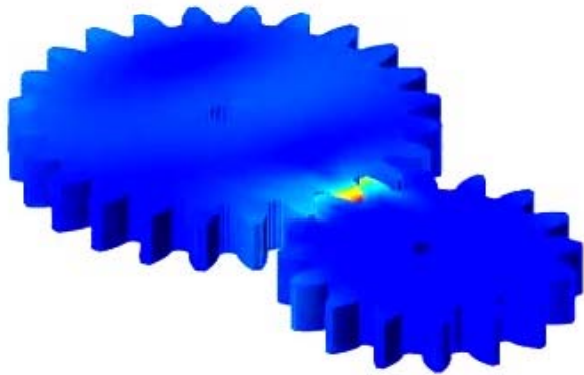
(Lundvall, Strömberg, Klarbring, 2004)

- 1 boundary node per tooth flank
100 internal vibrations modes
→ 695 DOFS \ll 480171 for FEM
- Parallel rotation axis → no misalignment
- Large center distance → significant backlash
- At $t=0s$, $\omega_1 = -1000$ rpm , $\omega_2 = 667$ rpm
- For $t > 0s$: Viscous torque: $T_1 = -1 \omega_1$; $\omega_2 = 667$ rpm
- Time step: $h=1E.-6s$



Eigenfrequencies of internal vibration modes (Hz)		
	pinion	gear
f_1	19520	10402
f_{100}	146068	115469

Gear system simulation



Co-simulation

Objectives

- Coupling between standard MBD and FEA softwares.
- Co-simulation of mechatronic systems.
- « Domain decomposition » of very large problems for parallel processing → multi-model solution.

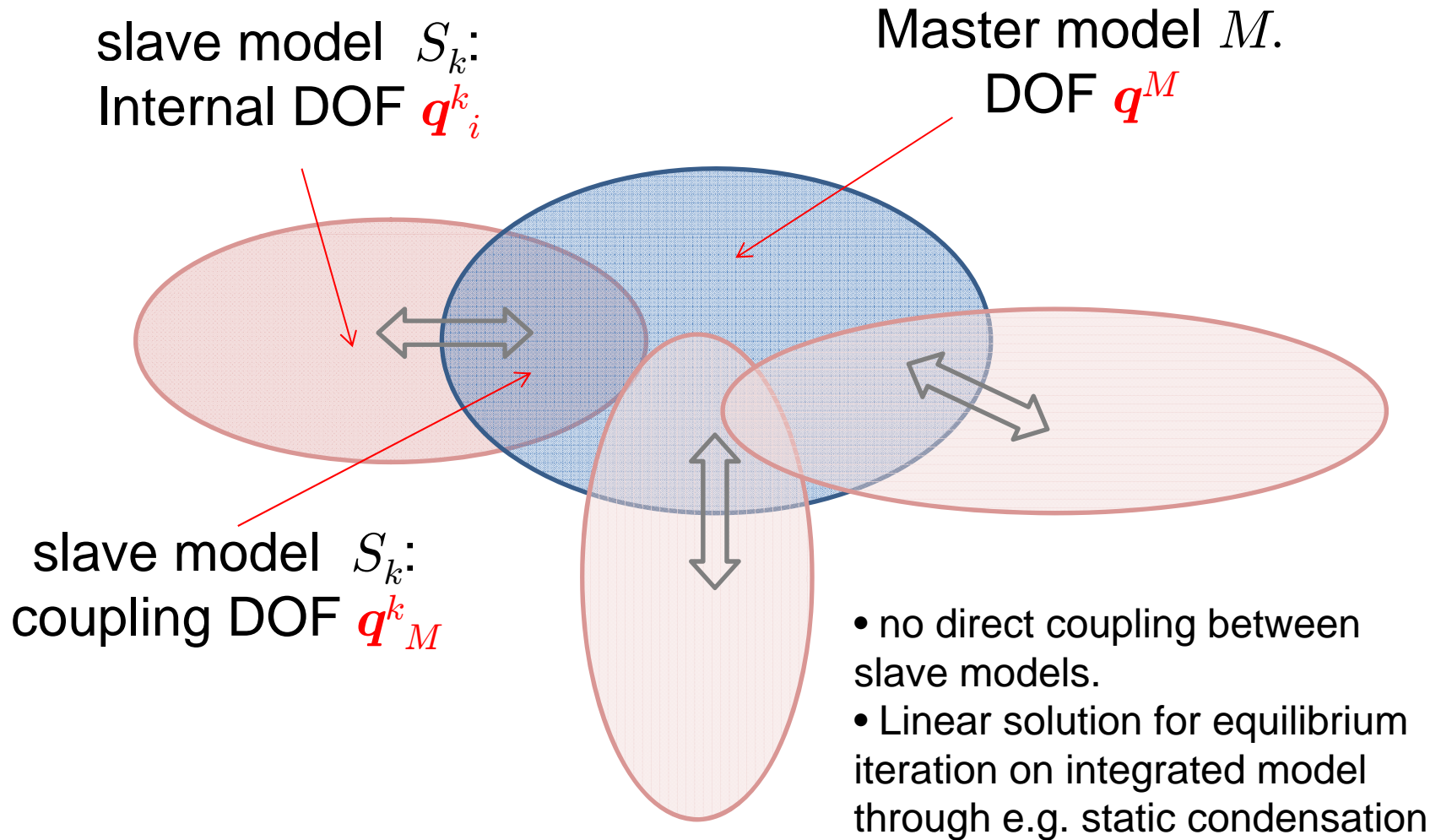
Methodology

- Generally based on the master / slave concept
- Different coupling levels can be envisaged, depending upon the nature of coupled systems and degree of accuracy of final solution.

Example of multi-model solution

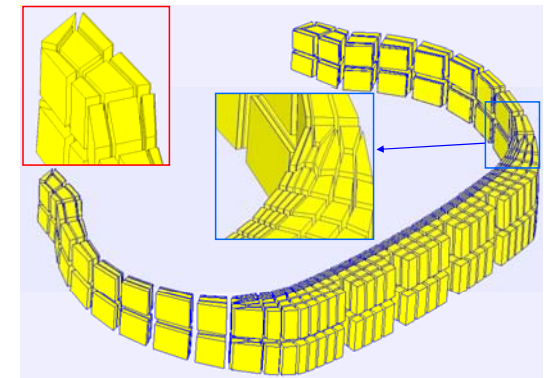
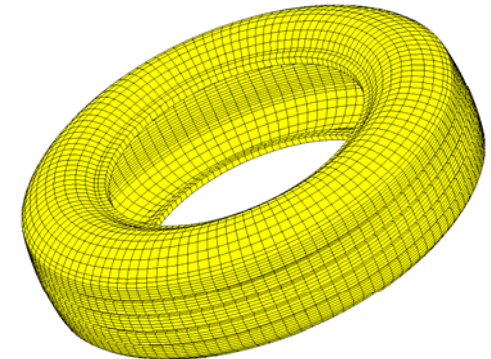
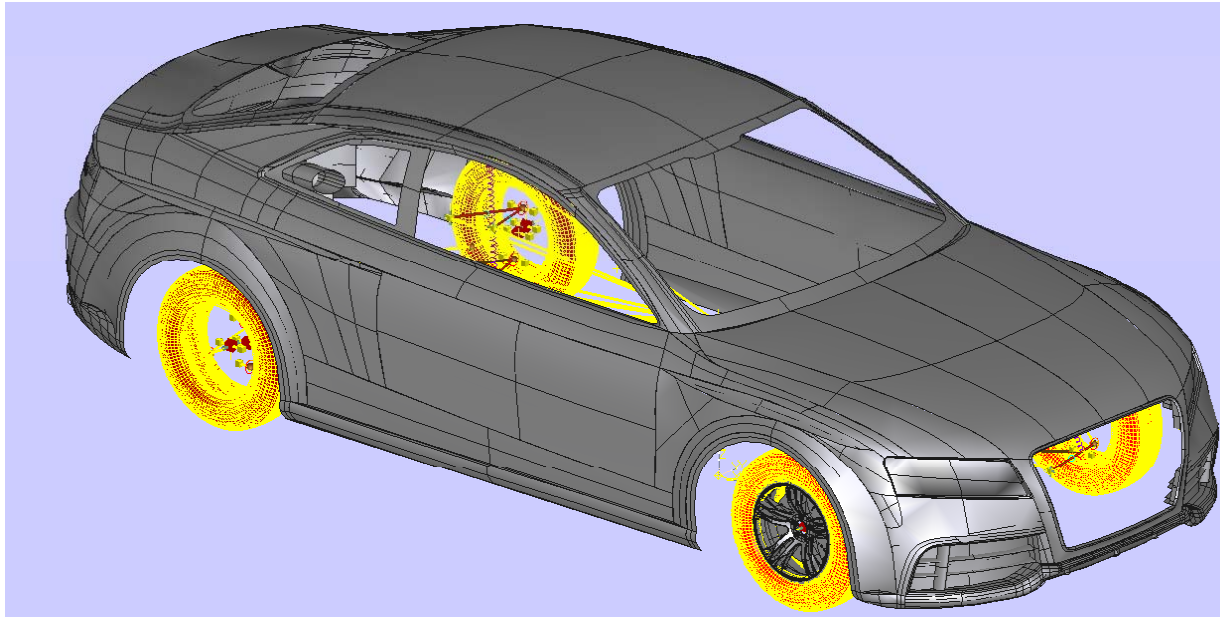
- vehicle dynamics simulation in higher frequency range → requires detailed modeling of critical components (e.g. coil springs, torsion bar, tires).
- Necessarily implies fully coupled solution.

Principle of multi-model solution



Example: MBD car model with FE tire models

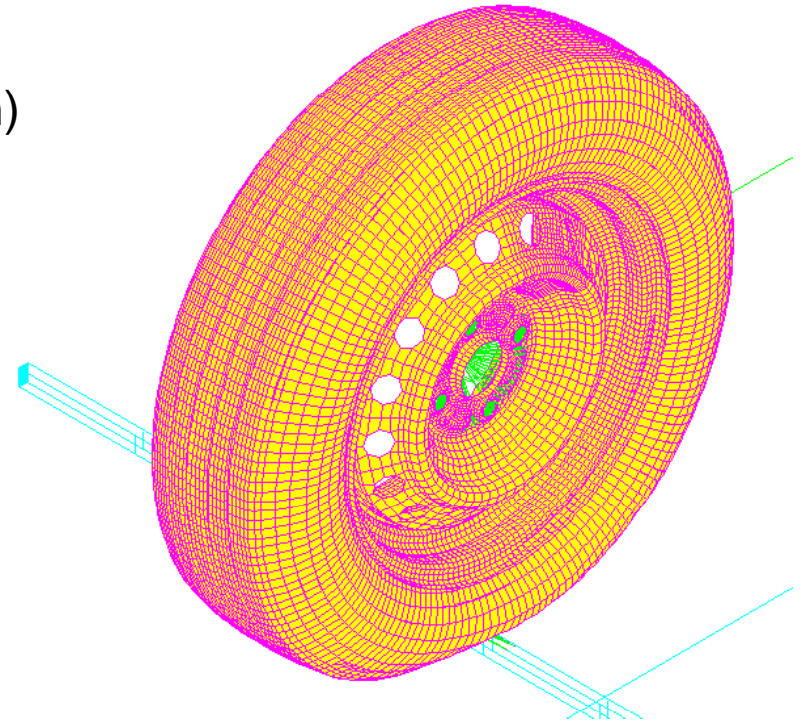
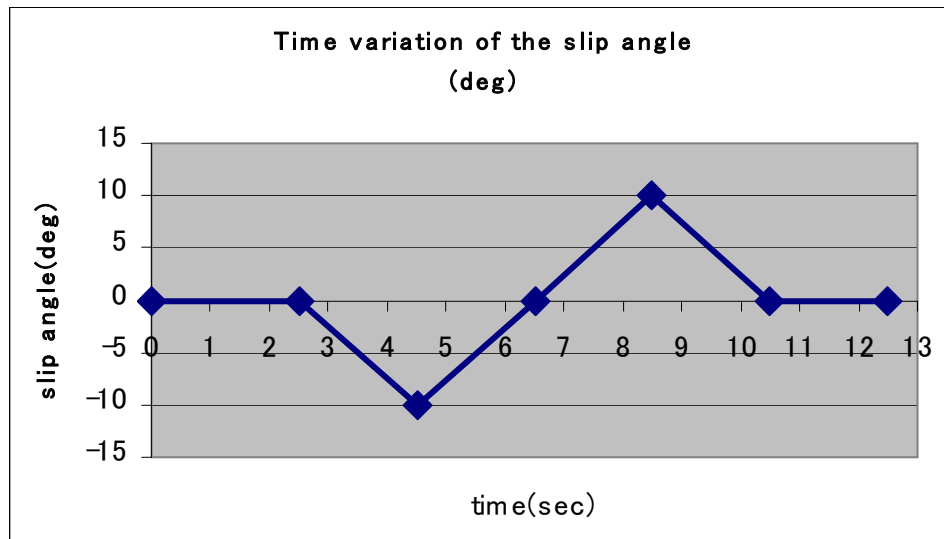
- Car body: rigid.
- Tires and twist beam: FE models.
- $\sim 2 \cdot 10^6$ DOF.



Objective: to capture high frequency response to road roughness.

FEA tire equipped car model

- ❑ 2 validation rides at 60 km/h
 - Straight ride with imposed variations of the slip angle
 - Straight ride over a comfort obstacle
- ❑ Simulation done in 3 phases
 - Static equilibrium (gravity + tire inflation)
 - Kinematics (initial velocity field)
 - Dynamic ride



Straight ride with slip angle variation

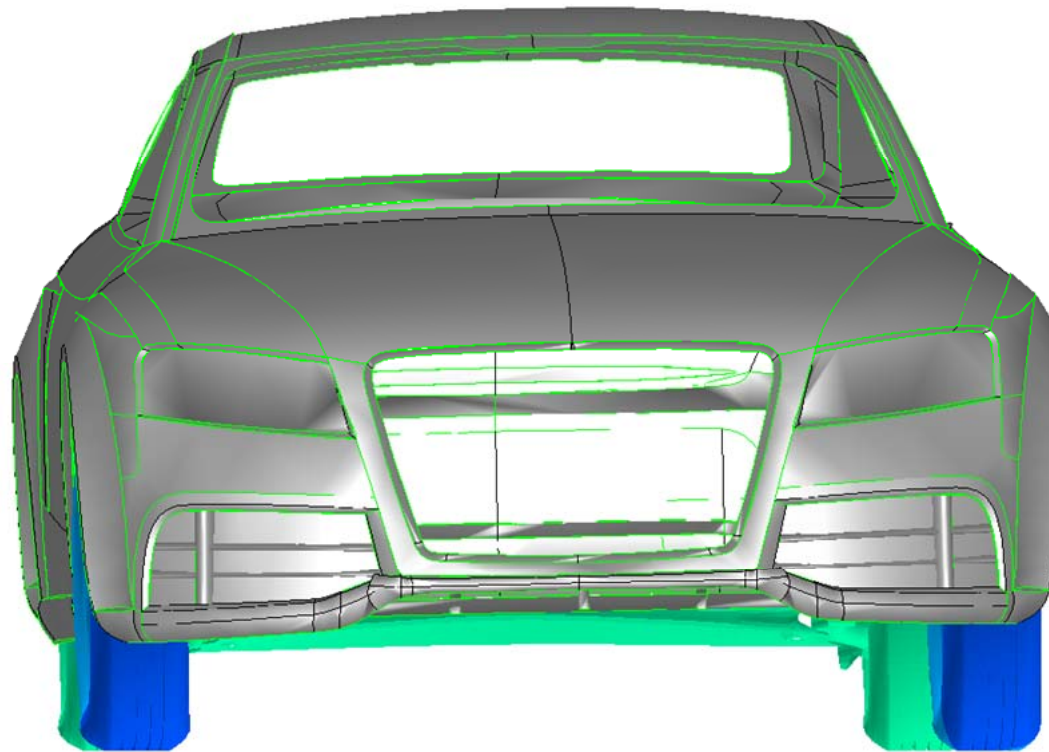


Figure 6. lateral displacement during slalom ride (front view)

Solution / multi-level solution accuracy

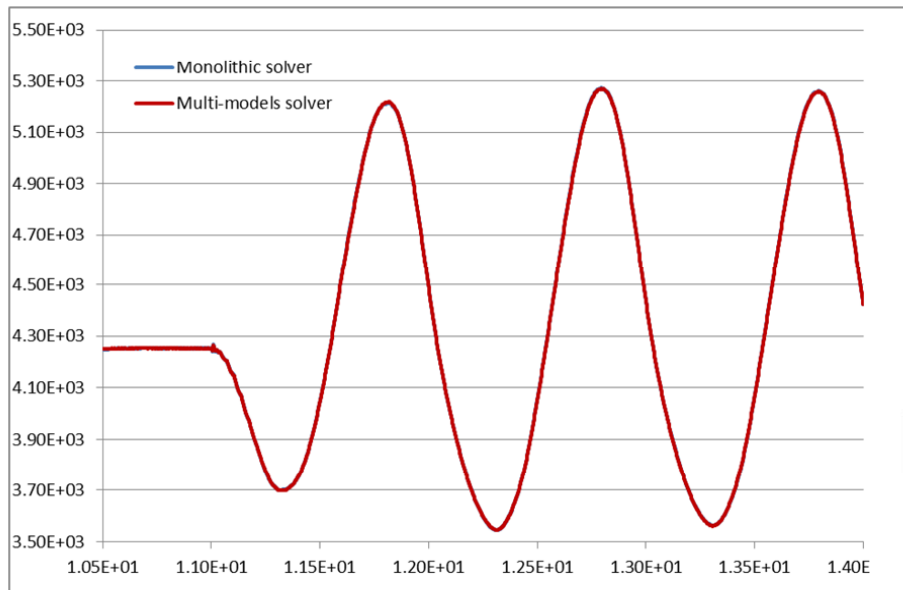


Figure 7. Magnitude of the force transmitted by the front left wheel

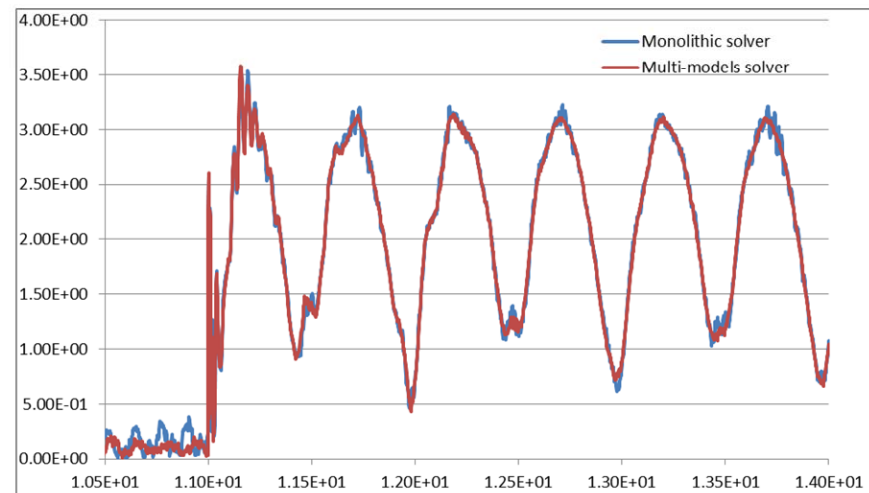


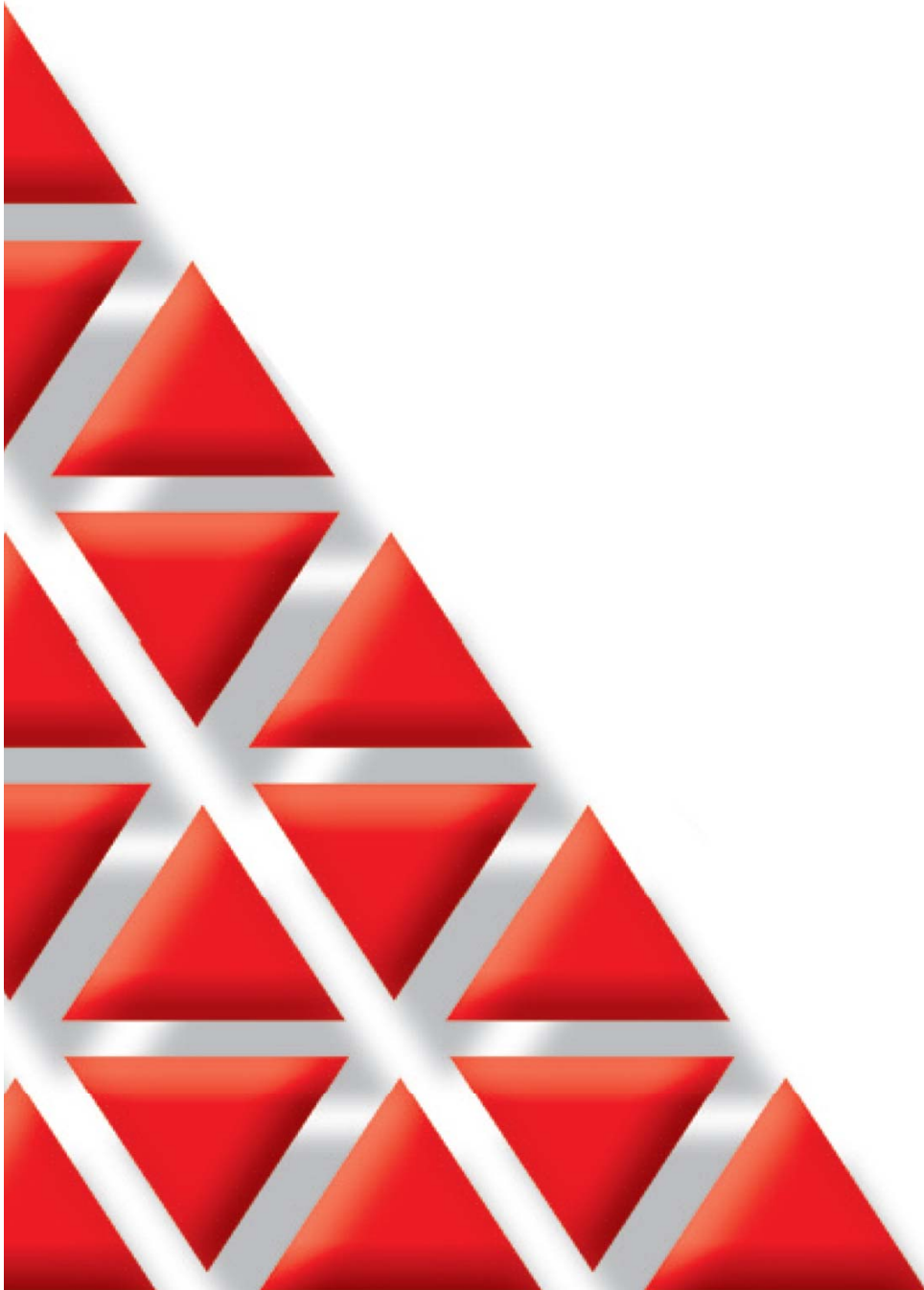
Figure 8. Global acceleration at front left wheel center

Computation performance

<i>models</i>	<i>Nr of iterations (linear system solutions)</i>	<i>Iteration cost ratio</i>	<i>Total Cost ratio</i>
1 model (6 Proc)	9087	1	1
1 model (12 Proc)	9087	0.62	0.66
1 model (24 proc)	9087	0.69	0.79
Multi-model (4 slave models, 25 proc)	7787	0.29	0.25
Multi-model (5 slave models, 26 proc)	7800	0.23	0.22

Conclusions

- ❑ FEA-MBD integration: not a dream, but a reality.
- ❑ Complexity of problems being addressed continuously increasing due to progress both in physical model quality, computer technology and numerical methods.
- ❑ Numerous topics still open for possible progress (e.g. contact/impact & friction, post-processing, computing performance).



Thank you !

